



Evidence from diatom-bound nitrogen isotopes for subarctic Pacific stratification during the last ice age and a link to North Pacific denitrification changes

Brigitte G. Brunelle,¹ Daniel M. Sigman,¹ Mea S. Cook,² Lloyd D. Keigwin,² Gerald H. Haug,³ Birgit Plessen,³ Georg Schettler,³ and Samuel L. Jaccard⁴

Received 18 August 2005; revised 27 July 2006; accepted 26 October 2006; published 2 March 2007.

[1] In a piston core from the central Bering Sea, diatom microfossil-bound N isotopes and the concentrations of opal, biogenic barium, calcium carbonate, and organic N are measured over the last glacial/interglacial cycle. Compared to the interglacial sections of the core, the sediments of the last ice age are characterized by 3‰ higher diatom-bound $\delta^{15}\text{N}$, 70 wt % lower opal content and 1200 ppm lower biogenic barium. Taken together and with constraints on sediment accumulation rate, these results suggest a reduced supply of nitrate to the surface due to stronger stratification of the upper water column of the Bering Sea during glacial times, with more complete nitrate consumption resulting from continued iron supply through atmospheric deposition. This finding extends the body of evidence for a pervasive link between cold climates and polar ocean stratification. In addition, we hypothesize that more complete nutrient consumption in the glacial age subarctic Pacific contributed to the previously observed ice age reduction in suboxia and denitrification in the eastern tropical North Pacific by lowering the nutrient content of the intermediate-depth water formed in the subpolar North Pacific. In the deglacial interval of the Bering Sea record, two apparent peaks in export productivity are associated with maxima in diatom-bound and bulk sediment $\delta^{15}\text{N}$. The high $\delta^{15}\text{N}$ in these intervals may have resulted from greater surface nutrient consumption during this period. However, the synchronicity of the deglacial peaks in the Bering Sea with similar bulk sediment $\delta^{15}\text{N}$ changes in the eastern Pacific margin and the presence of sediment lamination within the Bering Sea during the deposition of the productivity peaks raise the possibility that both regional and local denitrification worked to raise the $\delta^{15}\text{N}$ of the nitrate feeding Bering Sea surface waters at these times.

Citation: Brunelle, B. G., D. M. Sigman, M. S. Cook, L. D. Keigwin, G. H. Haug, B. Plessen, G. Schettler, and S. L. Jaccard (2007), Evidence from diatom-bound nitrogen isotopes for subarctic Pacific stratification during the last ice age and a link to North Pacific denitrification changes, *Paleoceanography*, 22, PA1215, doi:10.1029/2005PA001205.

1. Introduction

[2] Large regions of the high-latitude ocean, the Antarctic and the subarctic North Pacific in particular, are characterized by high phytoplankton productivity and incomplete consumption of the major nutrients nitrate and phosphate in the surface. During much of the last ice age, however, biological export production in both the Antarctic and the subarctic Pacific, including the Bering and Okhotsk Seas, was considerably lower than during the interglacial [Mortlock *et al.*, 1991; Kumar *et al.*, 1995; Francois *et al.*, 1997; Narita *et al.*, 2002; Kienast *et al.*, 2004; Jaccard *et al.*, 2005; Okazaki *et al.*, 2005a, 2005b]. The central question currently at hand is

whether this decline in productivity was associated with less complete consumption of the gross nutrient supply by phytoplankton [Elderfield and Rickaby, 2000; Anderson *et al.*, 2002], such as might result from a deeper mixed layer or pervasive summertime ice cover, or with a reduction in the gross nutrient supply itself, such as would result from a decrease in the exchange of nutrient-rich deep water with the surface [Francois *et al.*, 1997]. Distinguishing between these two hypotheses has important implications for understanding how the high-latitude ocean both responds to and mediates climate change.

[3] The N isotopes have the potential to distinguish between such alternative causes of past productivity changes in the polar ocean. Phytoplankton preferentially assimilate ^{14}N nitrate [Pennock *et al.*, 1996; Waser *et al.*, 1998], leaving surface water nitrate enriched in ^{15}N [Wu *et al.*, 1997; Sigman *et al.*, 1999b]. Because nitrate is the ultimate N source for phytoplankton in nutrient-rich surface waters, the degree of elevation in the $^{15}\text{N}/^{14}\text{N}$ of surface nitrate is paralleled by the $^{15}\text{N}/^{14}\text{N}$ of organic nitrogen produced in the surface ocean and exported as sinking organic matter [Altabet and Francois, 1994; Altabet and Francois, 2001; Lourey *et al.*, 2003]. Thus the degree of

¹Department of Geosciences, Princeton University, Princeton, New Jersey, USA.

²Department of Marine Geology and Geophysics, Woods Hole Oceanographic Institution, Woods Hole, Massachusetts, USA.

³Geoforschungszentrum Potsdam, Potsdam, Germany.

⁴Department of Earth and Ocean Sciences, University of British Columbia, Vancouver, British Columbia, Canada.

nitrate utilization occurring in the surface ocean is regionally correlated with the $\delta^{15}\text{N}$ of N sinking out of the euphotic zone and accumulating in the sediments [Altabet and Francois, 1994; Farrell et al., 1995; Francois et al., 1997] ($\delta^{15}\text{N} = \{[(^{15}\text{N}/^{14}\text{N}_{\text{sample}})/(^{15}\text{N}/^{14}\text{N}_{\text{reference}})] - 1\} \times 1000$, where the reference is atmospheric N_2).

[4] The use of the N isotopes to understand the implications of reduced polar productivity during the last ice age began largely in the Antarctic [Francois et al., 1997; Sigman et al., 1999a]. These and more recent N isotope studies in the region suggest that the decline in productivity was associated with reduced communication of nutrient-rich deep waters with the surface [Crosta and Shemesh, 2002; Robinson et al., 2004]. Specifically, while glacial export production was lower, the degree of nitrate consumption was either higher or unchanged, suggesting less gross nitrate supply to the surface. However, the N isotope evidence suggesting that the degree of nitrate consumption was not pervasively greater across the glacial Antarctic (i.e., one Atlantic record shows no clear glacial/interglacial change [Robinson et al., 2004]) complicates the interpretation, requiring that we consider the controls on major nutrient consumption in the polar ocean.

[5] The incomplete consumption of the major nutrients nitrate and phosphate in the modern Antarctic is often attributed to iron limitation [Martin et al., 1990; Moore et al., 2000], although light is also a potentially limiting resource. From this perspective, an increase in the completeness of nitrate consumption requires an increase in the iron-to-nitrate ($\text{Fe}:\text{NO}_3^-$) supply ratio. Upwelling from the ocean interior supplies both Fe and NO_3^- to the surface layer, while atmospheric inputs typically supply Fe in a much higher ratio to bioavailable N. Thus an increase in the $\text{Fe}:\text{NO}_3^-$ supply ratio in the Antarctic, such as would drive higher nitrate consumption during the last ice age, would likely require an increase in the relative importance of atmospheric Fe input, by increasing the atmospheric input and/or decreasing the deep water input. In the modern Antarctic, it appears that nearly all of the iron supply is from below [Archer and Johnson, 2000; Parekh et al., 2004]. As a result, model simulations suggest that a remarkably large increase in dust supply would be required to significantly raise the $\text{Fe}:\text{NO}_3^-$ supply ratio, even with reduced surface deep communications [Lefevre and Watson, 1999]. From this perspective, stratification of the Antarctic during the last ice age, if it occurred, might have failed to drive a pervasive increase in the degree of nitrate consumption [Robinson et al., 2004].

[6] Glacial/interglacial reconstructions of export production in the subarctic North Pacific indicate great similarity to the Antarctic [Gorbarenko, 1996; Narita et al., 2002; Sato et al., 2002; Nürnberg and Tiedemann, 2004; Jaccard et al., 2005; Okazaki et al., 2005a, 2005b], suggesting that a common mechanism operated in these two regions to produce the observed changes. Jaccard et al. [2005] have recently argued that this mechanism is the development of a more strongly stratified water column associated with global cooling, as has been posed for the Antarctic. However, in contrast to the Antarctic, the modern subarctic Pacific receives a significant fraction of its iron via aerial deposition [Martin and Gordon, 1988; Fung et al., 2000]. Given this

situation, if stratification were to reduce the gross nutrient supply in this region, one would expect a more robust increase in the $\text{Fe}:\text{NO}_3^-$ supply ratio than in the Antarctic, yielding a higher degree of nitrate consumption during glacial times. This work employs the nitrogen isotopes, as well as a suite of other paleoceanographic proxies, to test this hypothesis for the subarctic Pacific, both in its own right and as it relates to the paleoceanographic data from the Antarctic.

[7] The degree of nutrient utilization in surface waters is not the only signal that may contribute to changes in down core N isotope records; changes in the $\delta^{15}\text{N}$ of source nitrate will also influence these records. In the eastern Pacific, in particular, the $\delta^{15}\text{N}$ of nitrate upwelled to the surface may be higher than the ocean mean of $\sim 5\text{‰}$ [Sigman et al., 2000], due to exchange with zones of water column denitrification [Cline and Kaplan, 1975; Liu and Kaplan, 1989]. Denitrification, the dissimilatory reduction of nitrate to gaseous N_2 by bacteria, occurs where oxygen concentrations are too low to support rapid oxic respiration of organic matter (roughly less than $5 \mu\text{M}$) [Codispoti et al., 2001]. During denitrification, bacteria preferentially remove ^{14}N nitrate, leaving the residual nitrate pool enriched in ^{15}N [Barford et al., 1999, and references therein]. Some of this high $^{15}\text{N}/^{14}\text{N}$ nitrate is eventually mixed into the surface ocean and taken up by biota, which then transmit the high $^{15}\text{N}/^{14}\text{N}$ signal to the sediments. Water column denitrification occurs primarily in three regions of the ocean today: the eastern tropical North Pacific (ETNP), the eastern tropical South Pacific, and the Arabian Sea. As previous studies have shown that ^{15}N -enriched nitrate from the ETNP does in fact propagate northward along the eastern edge of the Pacific [Liu and Kaplan, 1989; Altabet et al., 1999; Kienast et al., 2002; Sigman et al., 2003], changes in subsurface nitrate $\delta^{15}\text{N}$ will have to be considered when interpreting a paleoceanographic record of sedimentary $\delta^{15}\text{N}$ from the subarctic Pacific.

[8] Isotopic studies of bulk sedimentary nitrogen in open ocean settings are complicated by diagenetic processes occurring in the sediments, which tend to raise the $\delta^{15}\text{N}$ of the preserved organic matter. Studies of sediments from modern productive, continental margin environments find no evidence for an effect [Altabet et al., 1999; Thunell et al., 2004]. In contrast, open ocean studies have observed clear enrichments of as much as 5‰ [Altabet and Francois, 1994; Altabet, 1996; Sachs et al., 1999], and downcore changes in this effect are likely.

[9] To avoid the concern of diagenetic alteration, a growing body of paleoceanographic work is focusing on the organic matter internal to microfossils, with most work to date involving the siliceous frustules of diatoms [Shemesh et al., 1993; Sigman et al., 1999a; Crosta and Shemesh, 2002; Crosta et al., 2002; Robinson et al., 2004, 2005]. This organic matter appears to be native to the diatoms and protected from early bacterial diagenesis [King, 1977; Swift and Wheeler, 1992; Kröger et al., 2000; Ingalls et al., 2003; Poulsen et al., 2003; Ingalls et al., 2004]. Here, we further the development of this paleoceanographic measurement and apply it to a sediment record from the central Bering Sea, one of the more nutrient-rich regions of

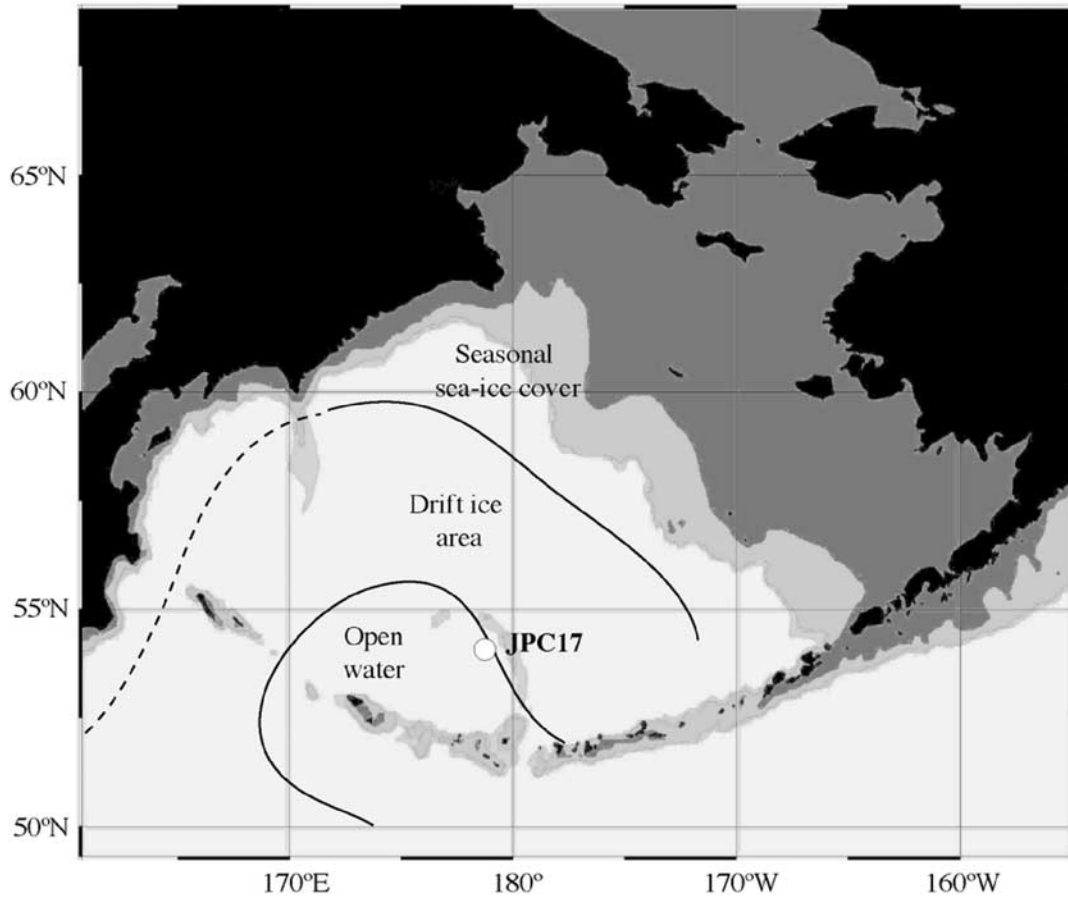


Figure 1. Map showing location of piston core JPC17. This site (53.9330°N , 178.6988°E) is on the western flank of Bowers Ridge at 2209 m depth and is protected from turbidites from the Alaskan shelf and slope. Dark gray area represents the aerially exposed paleocontinental shelf during the LGM due to a 100 m lowering of sea level. Light gray area represents paleobathymetry from 0 to 900 m. Lines illustrate approximate boundaries between regions of seasonal sea ice cover, drift ice, and open water during the LGM. The map and all ice age features are redrawn from *Katsuki and Takahashi* [2005] with permission from Elsevier.

the subarctic North Pacific. We report $\delta^{15}\text{N}$ records of both diatom microfossil-bound N ($\delta^{15}\text{N}_{\text{db}}$) and bulk sedimentary N, considering the influences of both nitrate consumption in the surface and the isotopic composition of the subsurface nitrate supply. We also report sedimentary concentrations and accumulation rates of biogenic barium (Ba_{bio}), opal, nitrogen, and CaCO_3 , which we interpret in terms of the productivity of the region.

2. Materials

[10] The sediments studied in this work were collected during a cruise in June–July 2002 aboard the USCG *Healy* (Healy 0202) and are archived at the Woods Hole Science Center’s Core and Sediment Archive. Piston core JPC17 was retrieved from the southwestern flank of Bowers Ridge (53.9330°N , 178.6988°E , 2209 m; Figure 1). This site in the central Bering basin is protected from turbidites from the Alaskan continental margin that have been found to compromise records recovered from the deep seafloor northeast

of Bowers [*Nakatsuka et al.*, 1995]. The basic chronology of the record is given by foraminiferal $\delta^{18}\text{O}$ stratigraphies of the planktonic species *Neogloboquadrina pachyderma* (sinistral) and of the benthic genus *Uvigerina*, as well as by seven radiocarbon dates (measured on *N. pachyderma* (s.) $>150\ \mu\text{m}$) [*Cook et al.*, 2005; additional data]. Radiocarbon dates were converted into calendar years using Calib5.0.1 (<http://radiocarbon.pa.qub.ac.uk/calib>), (*Stuiver et al.* [1998] using $\Delta R = 300$ year, corresponding to a ~ 700 year reservoir correction); corrections for dates >21.4 ka were estimated using the results of *Hughen et al.* [2004] (see auxiliary Table S1 for uncorrected and calibrated ages).¹ No correction is applied to the radiocarbon date at 49,100 years as the error is significant (640 year 1SD) and the atmospheric ^{14}C record is poorly constrained at this time. Average sedimentation rates calculated for intervals

¹Auxiliary material data sets are available at <ftp://ftp.agu.org/apend/pa/2005pa001205>. Other auxiliary material files are in the HTML.

between ^{14}C -dated layers are ~ 15 cm/kyr during the Holocene and ~ 12 cm/kyr during the Last Glacial Maximum. On the basis of extrapolation of measured accumulation rates in the upper part of the core, and consistent with the variations in opal, biogenic barium content, and $\delta^{15}\text{N}_{\text{db}}$, JPC17 appears to extend back to the interglacial conditions of early stage 5.

[11] “Green layers” rich in organic matter, CaCO_3 , and biogenic opal characterize the Bølling-Allerød and early Holocene in this core. These layers are well correlated with laminated intervals in shallower cores from the Bering slope, which indicate middepth suboxia in the Bering Sea at these times [Cook *et al.*, 2005]. The remainder of JPC17 is extremely poor in CaCO_3 (generally less than 5%), whereas opal content tends to vary somewhat systematically with $\delta^{18}\text{O}$, with interglacials characterized by higher opal content.

3. Methods

[12] The isotopic composition of diatom-bound organic N was determined using the method described by Robinson *et al.* [2004, 2005], but with modifications to the chemical cleaning of the diatom microfossils. The method detailed by Robinson *et al.* [2004] (R04 below) involves (1) physical separation of the diatom fraction from the bulk sediment [Sigman *et al.*, 1999a], (2) removal of labile organic matter coating the diatom frustules by oxidation with hydrogen peroxide, (3) conversion of organic nitrogen to NO_3^- by persulfate oxidation [Knapp and Sigman, 2003], (4) measurement of NO_3^- concentration by chemiluminescence [Braman and Hendrix, 1989], and (5) conversion of NO_3^- to N_2O by the denitrifier method [Sigman *et al.*, 2001], with measurement of the isotopic composition of the N_2O by gas chromatography isotope ratio mass spectrometry using a modified ThermoFinnigan GasBench II and Delta Plus [Casciotti *et al.*, 2002]. Robinson *et al.* [2005] added a reductive cleaning step between steps 1 and 2 above (using dithionite-citric acid), as a precaution to prevent interference of metal oxides with the subsequent oxidative cleaning.

[13] We undertook our study of JPC17 realizing that these sediments may be problematic for the cleaning protocol of R04, which was designed for the relatively “clean”, high-opal sediments of the Southern Ocean. In that work, diatom opal extracted from clay-rich ($\sim 40\%$ opal) glacial Antarctic sediments proved more difficult to clean of external N than opal-rich Holocene material, requiring multiple refreshings of hydrogen peroxide to stabilize. While we do not know why the opal from clay-rich sediments is more difficult to clean, it likely involves diagenetic alteration of the frustule surfaces (H. Ren, unpublished data, 2006). For much of the glacial section of JPC17, opal content is between 20 and 40% by weight, and the sediments are more difficult to physically separate than are Southern Ocean materials, suggesting a greater degree of diagenetic reaction between the opal and aluminosilicates. Thus we were suspicious that the peroxide cleaning protocol would not be sufficient in the glacial section of JPC17.

[14] Indeed, while measurements of $\delta^{15}\text{N}_{\text{db}}$ with the R04 protocol in opal-rich Holocene samples from JPC17 were highly reproducible, replicate cleanings of individual samples from the opal-poor sediments of the Last Glacial

Maximum (LGM) yielded exceedingly poor reproducibility (Figure 2). For several of these LGM samples, we applied additional refreshings with hydrogen peroxide to test whether a consistent isotope value could eventually be obtained, with mixed results. Similarly, the addition of the reductive cleaning step during our tests of the peroxide cleaning appeared to improve the results only moderately (results not shown).

[15] In cleaning tests by R04, boiling perchloric acid yielded a harsher cleaning than did peroxide, although with clear evidence for occasional alteration of the diatom-bound N in opal-rich samples, yielding sporadically higher $\delta^{15}\text{N}_{\text{db}}$. On the basis of those results, we tested oxidative cleaning by heating the sample with $\sim 55\%$ perchloric acid until boiling. This approach is very similar to the “perchloric soft” treatment applied by R04, which generated good reproducibility for more clay-rich samples from the Antarctic. Indeed, this yielded much more consistent results for samples from the clay-rich LGM section of JPC17 (Figure 2). However, as was feared based on the results of R04, this protocol yielded occasional high- $\delta^{15}\text{N}_{\text{db}}$ “flyers,” perhaps more frequently in the more opal-rich Holocene samples (Figure 2). We then tried a gentler perchloric cleaning, in which samples in $\sim 55\%$ perchloric acid are heated at 100°C for 2 hours.

[16] The 100°C cleaning with perchloric acid compares well with the heat-until-boiling protocol, especially for the clay-rich LGM sediments (Figure 2). However, as we had hoped, the 100°C perchloric cleaning largely reproduces the results from peroxide cleaning in opal-rich Holocene sediments, in which peroxide has been shown previously to yield consistent and reproducible results (Figure 2; for higher opal sediments from deeper in the core, see auxiliary Figure S1). Moreover, the 100°C perchloric protocol lacks the sporadic high $\delta^{15}\text{N}_{\text{db}}$ measurements that occur with the boiling perchloric protocol. Reproducibility for individual samples with the 100°C perchloric protocol is 0.3% 1SD.

[17] In light of these experiments, our current cleaning protocol (and the protocol used here) is identical to that of Robinson *et al.* [2005], except that the boiling hydrogen peroxide step is replaced with a single application of hydrogen peroxide in a 100°C water bath for one hour (to consume extremely labile organic matter and any residual reducing capacity from the reductive cleaning) followed by a strong oxidative cleaning with perchloric acid in a 100°C water bath for 2 hours (see auxiliary material for complete protocol). This method has recently yielded excellent reproducibility and oceanographically consistent downcore trends in sediments with opal content as low as 10% (B.G. Brunelle, unpublished data, 2005).

[18] Biogenic opal concentration was determined using the method described by Mortlock and Froelich [1989]. Precision was generally better than 4 wt%.

[19] The content and isotopic composition of bulk sedimentary N were analyzed using an elemental analyzer (NC2500 Carlo Erba) coupled with a ConFlow III interface on a stable isotope ratio mass spectrometer (ThermoFinnigan DELTA + XL) at the GeoForschungsZentrum in Potsdam, Germany. Replicate analyses indicated a standard deviation of 0.2% for $\delta^{15}\text{N}$ and 0.007 wt % for N content.

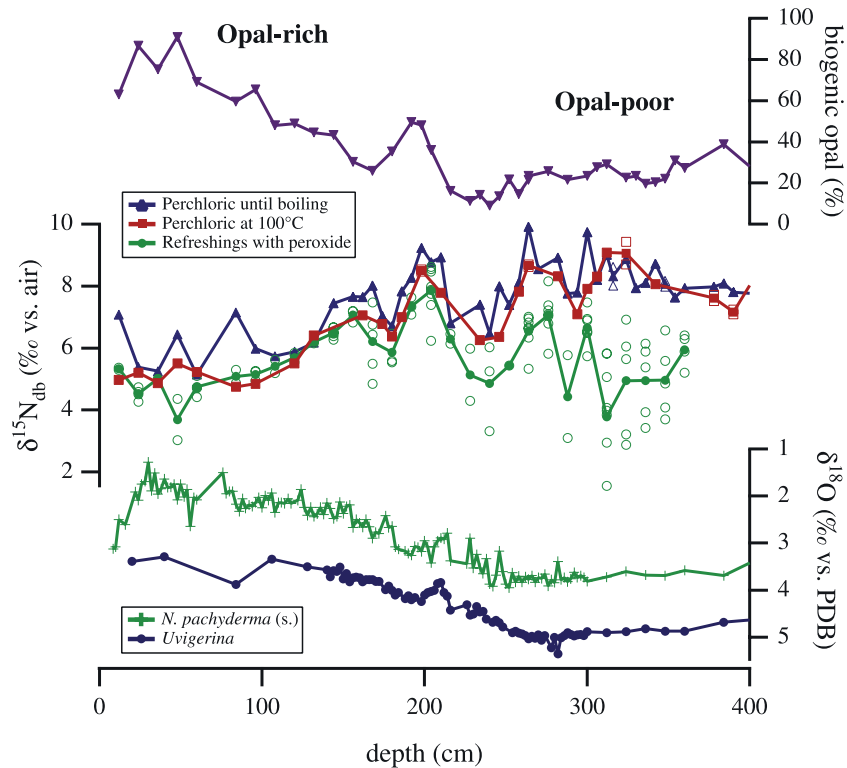


Figure 2. Comparison of $\delta^{15}\text{N}_{\text{db}}$ as measured following three different oxidative cleaning protocols on a suite of samples through the LGM in JPC17. In the “perchloric until boiling” and “perchloric at 100°C” profiles, open symbols are replicates for the entire protocol, including the physical opal extraction and wet chemical cleaning steps; solid symbols are single measurements or averages of two or more replicates. In the “refreshings with peroxide” profile, open symbols indicate samples that underwent multiple peroxide cleanings, but which were not necessarily extracted separately; solid symbols are the average for all replicates. Cleaning with perchloric acid at 100°C is the basis of our current protocol, which is used for all analyses in subsequent figures.

[20] Major and trace elements were analyzed by ICP-AES (IRIS, Thermo Elemental). Digestion of 0.25 g sample aliquots, as applied in the GFZ laboratory, includes (1) carbonate dissolution and wet oxidation of organics (HNO_3 , 3 h, 130°C), (2) oxidation of refractory organic compounds (HClO_4 , 5 h, 160°C), (3) silicate dissolution (HF , 2 days, 70°C), (4) treatment with HClO_4 (2 h, 210°C), and (5) addition of HCl and final dissolution to a volume of 50 mL. Acid concentrations and the typical major element matrix of the final digestion solutions were considered for the preparation of the multielement standard solutions. The mean relative standard deviation for the measurement of Ba, Ca, and Al is below 1%. Analytical uncertainty can be slightly above 1% due to variable matrix composition. Biogenic barium was calculated by assuming a constant detrital Ba/Al ratio of 0.0075 ($\text{Ba}_{\text{bio}} = \Sigma\text{Ba} - 0.0075 \text{ Al}$) [Dymond *et al.*, 1992].

[21] Average ^{14}C -derived accumulation rates were calculated by multiplying the sedimentation rate, the average concentration of the biogenic component, and the average dry bulk density between depths with ^{14}C measurements. Sedimentation rates were determined by linearly interpolating between calibrated radiocarbon dates (the core top was assigned an age of 0 ka, an assumption that is corroborated

by the agreement between average ^{14}C -derived and average Th-normalized fluxes for the Holocene). Wet bulk density was determined from shipboard measurements of gamma ray attenuation in JPC17, and dry bulk density was then determined by assuming a bulk grain density weighted for opal content (bulk grain density = $(2.1 \text{ g/cm}^3 \times \text{opal fraction}) + (2.7 \text{ g/cm}^3 \times (1 - \text{opal fraction}))$).

[22] Th-normalized fluxes were calculated from measurements of Th excess activity according to Francois *et al.* [2004]. The ^{230}Th was measured at University of British Columbia by isotopic dilution using ^{229}Th spike on a single collector, sector field ICP-MS, following the procedure described by Choi *et al.* [2001]. Briefly, the sediment samples were spiked and equilibrated with ^{229}Th prior to total digestion in HNO_3 , HF and HClO_4 . An aliquot was analyzed directly for ^{232}Th and ^{238}U using ^{229}Th and ^{236}U spikes, respectively. The remaining solution was used for ^{230}Th separation by anion-exchange resins (AG1-X8) and subsequently analyzed by ICP-MS in low-resolution mode. Initial excess activities ($^{230}\text{Th}_{\text{xs},0}$) were obtained after corrections for (1) the detrital ^{230}Th inferred from the ^{232}Th content of the sediment and using the average $^{238}\text{U}/^{232}\text{Th} = 0.7 \pm 0.1$ [Hendersen and Anderson, 2003] activity ratio of the lithogenic fraction of the sediment, (2) the decay since

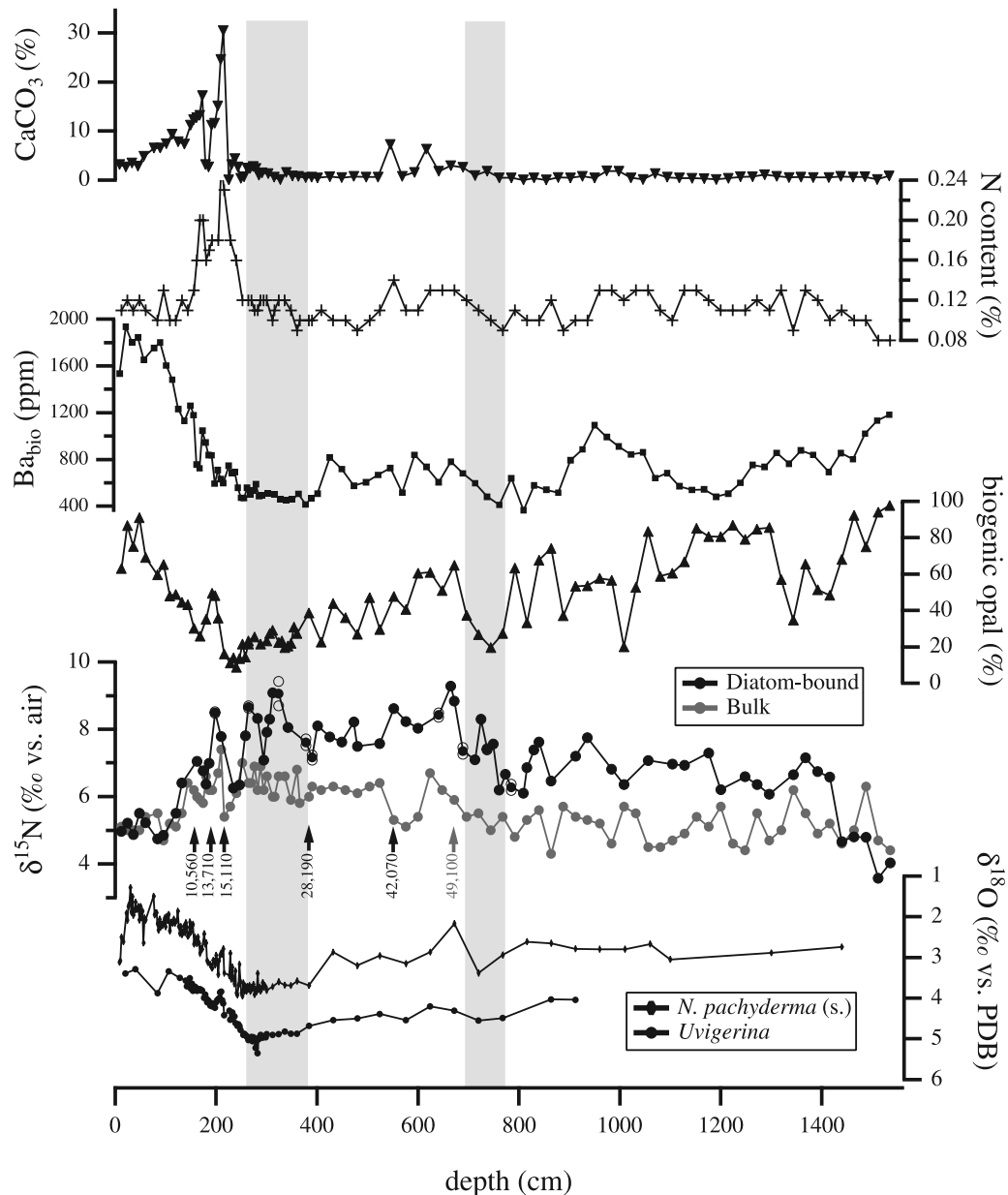


Figure 3. Downcore profile in JPC17 extending back to stage 5 of foraminiferal $\delta^{18}\text{O}$ (vs. PDB, measured on *N. pachyderma* (s.) and *Uvigerina*), $\delta^{15}\text{N}_{\text{db}}$, bulk sediment $\delta^{15}\text{N}$, biogenic opal content, biogenic barium, nitrogen content, and CaCO_3 content. Shaded areas indicate the LGM and stage 4 as inferred from the $\delta^{18}\text{O}$ stratigraphies, radiocarbon dates, and the record of opal content (see text). Five ^{14}C dates are given in calendar years [Cook *et al.*, 2005; additional data]; the oldest date at 49,100 years remains in radiocarbon years (see text).

the time of sediment deposition estimated from the age model, and (3) the diagenetic addition of ^{230}Th derived from authigenic U.

4. Results

4.1. Productivity Proxies

[23] In JPC 17, the concentrations of biogenic opal and Ba_{bio} are higher in the Holocene interval than the last glacial

sediments (Figure 3), as are both the ^{14}C -derived and Th-normalized accumulation rates (Figure 4), consistent with other results from the subarctic North Pacific [Dymond *et al.*, 1992; Gorbarenko, 1996; Narita *et al.*, 2002; Sato *et al.*, 2002; Nürnberg and Tiedemann, 2004; Jaccard *et al.*, 2005; Okazaki *et al.*, 2005a, 2005b]. Given these results and because we have accumulation rate estimates only for the last 49 kyr, we use biogenic concentration data in the deeper part of the core to infer qualitative changes in productivity.

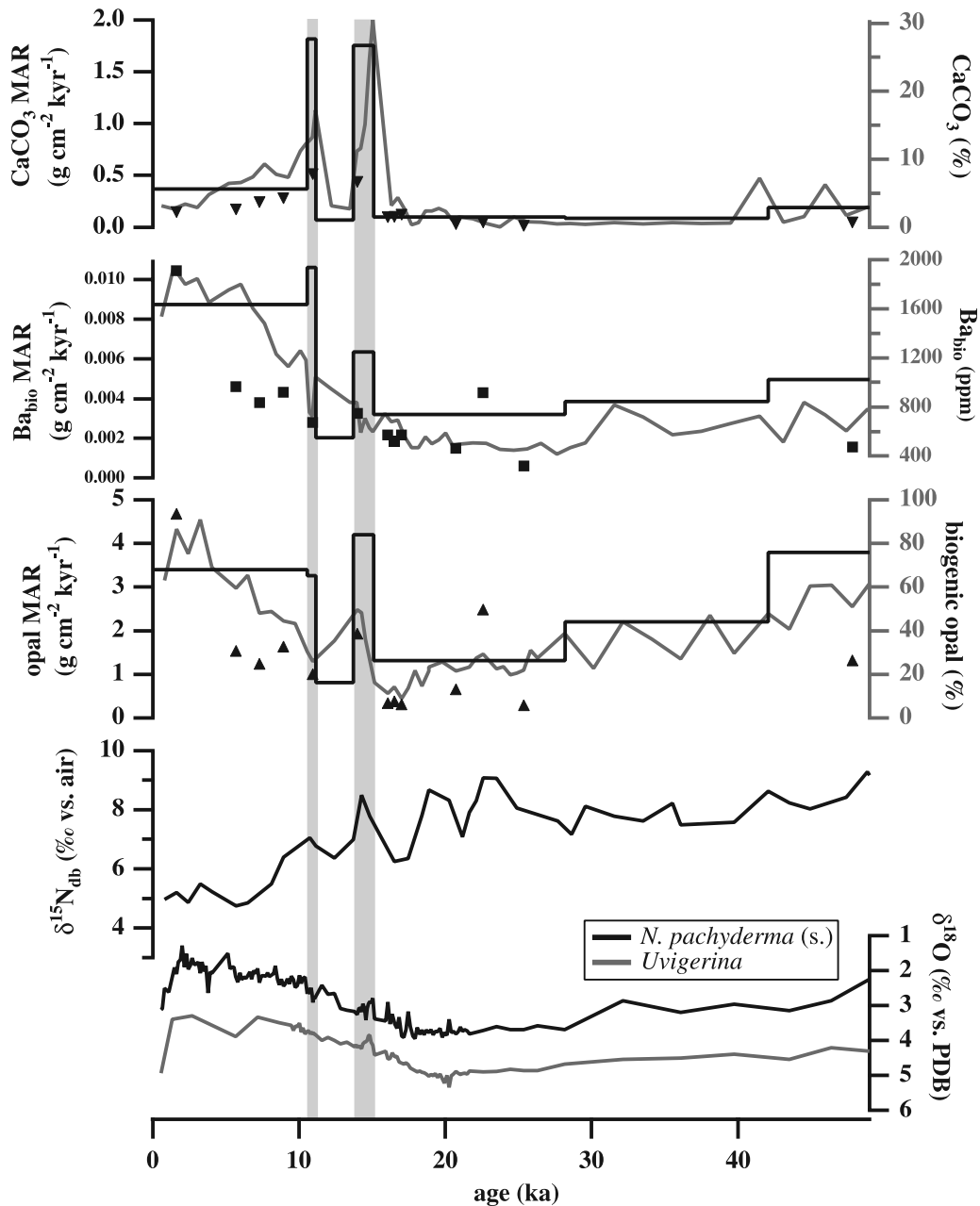


Figure 4. Downcore profile of foraminiferal $\delta^{18}\text{O}$ (versus PDB, measured on *N. pachyderma* (s.) and *Uvigerina*), $\delta^{15}\text{N}_{\text{db}}$, and biogenic opal, biogenic barium, and CaCO_3 concentration (gray lines), average ^{14}C -derived accumulation, and Th-normalized accumulation (points) versus age in JPC17. Shaded areas indicate “green layers,” which are correlated with laminated intervals in shallower cores from the Bering slope that occur during the Bølling-Allerød warm period and after the Younger Dryas [Cook *et al.*, 2005].

We also turn to CaCO_3 and N content and accumulation as additional potential indicators of productivity change, although the former is also influenced by deep ocean calcite saturation state and the latter represents a tiny residual of the sinking flux.

[24] On the basis of radiocarbon dates and reasonable extrapolations of sedimentation rate, we believe that the opal- and Ba_{bio} -rich interval at the base of the core represents early stage 5 interglacial conditions. In support of this, applying an

average glacial accumulation rate of 12.4 cm/kyr (determined for the radiocarbon-dated interval between 20 and 42 ka) to the remainder of the sediment record >49 ka yields a core bottom age of 119 ka. From this interval, opal and Ba_{bio} content decrease roughly in parallel to lowest levels in the LGM ($\sim 20\%$ and 450 ppm, respectively), before rising into the Holocene. The gradual glacial decline in opal content is punctuated by a coherent opal minimum at ~ 750 cm depth,

which may represent stage 4, qualitatively consistent with a slight maximum in foraminiferal $\delta^{18}\text{O}$.

[25] Previous work in the subarctic North Pacific has noted a dramatic and complex set of events during deglaciation and the early Holocene. A significant increase in productivity has been observed in the open western subarctic Pacific and the Okhotsk Sea during the Bølling-Allerød [Keigwin *et al.*, 1992; Ternois *et al.*, 2001; Sato *et al.*, 2002; Crusius *et al.*, 2004; Seki *et al.*, 2004]. In JPC17, Cook *et al.* [2005] note two “green layers” that correspond to laminated intervals in shallower cores from the Bering basin and that correspond to the Bølling-Allerød and early Holocene, separated by an interval corresponding to the Younger Dryas (Figure 4). These assignments are consistent with the radiocarbon dates for JPC17.

[26] At the end of the last glacial termination, opal and barium accumulation remain low for the earliest portion of deglaciation, when a rise in planktonic and benthic $\delta^{18}\text{O}$ is first discernable (~ 17.5 ka, Figure 4); in fact, the Th-normalized fluxes during this interval are among the lowest measured in the record, although these data are admittedly sparse. However, upon the deposition of the first green layer, opal, Ba_{bio} , and CaCO_3 deposition appear to increase, and this is repeated for the second green layer after the interval corresponding to the Younger Dryas (Figure 4). The Th-normalized flux estimates suggest relatively modest biogenic accumulation during this interval, while the average ^{14}C -derived accumulation data indicate significantly greater rates (1.9 and $4.2 \text{ g cm}^{-2} \text{ kyr}^{-1}$ for opal accumulation, respectively). While sediment focusing may affect the ^{14}C -derived accumulation rate, this subarctic Pacific-wide peak cannot be solely due to focusing [Crusius *et al.*, 2004]. It should also be noted that the Ba_{bio} peaks during green layers may be underestimates of Ba_{bio} accumulation due to barite dissolution associated with the demonstrably low O_2 conditions of the green layers [McManus *et al.*, 1998; Cook *et al.*, 2005]. Subsequently, both opal and Ba_{bio} accumulation increase gradually to their relatively high interglacial levels, the ^{14}C -derived and Th-normalized fluxes yielding similar estimates, while CaCO_3 decreases through the Holocene.

4.2. Isotopic Composition of Diatom Microfossil-Bound and Bulk Sedimentary N

[27] The record of $\delta^{15}\text{N}_{\text{db}}$ from JPC17 exhibits significant and coherent changes throughout the last glacial-interglacial cycle (Figure 3). In general, glacial conditions are characterized by high $\delta^{15}\text{N}_{\text{db}}$ (6.5–9‰), whereas full interglacial conditions are associated with low $\delta^{15}\text{N}_{\text{db}}$ (3.5–5.5‰). Early stage 5 values average 4.4‰, and then rise abruptly to ~ 6.7 ‰ as opal content drops. $\delta^{15}\text{N}_{\text{db}}$ increases steadily throughout the remainder of isotope stage 5 to ~ 7.3 ‰, and then decreases to ~ 6.2 ‰ upon what may be the onset of stage 4. By the end of the opal minimum attributed to stage 4, however, $\delta^{15}\text{N}_{\text{db}}$ has risen to 8.3‰. The transition between inferred stage 4 and 3 is marked by a decrease in $\delta^{15}\text{N}_{\text{db}}$ to ~ 7 ‰, followed by an abrupt rise to 9.3‰ at the beginning of stage 3. Stage 3 $\delta^{15}\text{N}_{\text{db}}$ then wanes slightly but remains high, with $\delta^{15}\text{N}_{\text{db}}$ increasing into the LGM and peaking at 9‰ during stage 2.

[28] As with the productivity-related parameters, there are dramatic changes in $\delta^{15}\text{N}_{\text{db}}$ across the deglacial transition (Figure 4). Immediately upon deglaciation, as indicated by the initial rise in benthic $\delta^{18}\text{O}$, $\delta^{15}\text{N}_{\text{db}}$ declines to ~ 6.3 ‰. While this initial deglacial change is indicated by only two samples in Figures 3 and 4, the same feature is also reproduced in the analyses generated with the alternative perchloric acid cleaning protocol (Figure 2), so we are confident that it is real. $\delta^{15}\text{N}_{\text{db}}$ then begins to rise abruptly at 15.1 ka to ~ 8.5 ‰ within the green layer associated with the Bølling-Allerød (Figure 4). This peak is followed by a decline in $\delta^{15}\text{N}_{\text{db}}$ into the Younger Dryas, after which another (albeit muted) peak occurs in the second green layer. Finally, $\delta^{15}\text{N}_{\text{db}}$ relaxes to ~ 5.1 ‰ with the onset of full interglacial conditions, similar to the low $\delta^{15}\text{N}_{\text{db}}$ interval at the base of the core that we have inferred to be early stage 5.

[29] On the large scale, $\delta^{15}\text{N}_{\text{db}}$ varies inversely with concentration and accumulation of opal (and of Ba_{bio} , Figures 3 and 4). However, some small-scale variations in $\delta^{15}\text{N}_{\text{db}}$ and opal content are positively correlated. Both the deglaciation and the apparent onset of stage 3 are marked by a return to high $\delta^{15}\text{N}_{\text{db}}$ and high opal content.

[30] Bulk nitrogen $\delta^{15}\text{N}$ follows a trend somewhat similar to $\delta^{15}\text{N}_{\text{db}}$: values are low during full-interglacial conditions and high during full glacial conditions (Figure 3). Likewise, the deglacial and early Holocene peaks in $\delta^{15}\text{N}_{\text{db}}$ described above are also apparent in the bulk $\delta^{15}\text{N}$ record. However, the progressive rise in $\delta^{15}\text{N}$ through the glacial is muted in the bulk sediment record: the average $\delta^{15}\text{N}$ difference between LGM and Holocene is only 1.5‰, compared to a difference of 3.5‰ in $\delta^{15}\text{N}_{\text{db}}$.

5. Interpretation

5.1. Cause of High Diatom-Bound $\delta^{15}\text{N}$ During the Last Ice Age

[31] In the modern open Bering Sea, the summertime nitrate drawdown is associated with ^{15}N enrichment of the residual mixed layer nitrate, due to isotope discrimination during nitrate assimilation and the export of organic N with a $\delta^{15}\text{N}$ lower than the nitrate supplied to the mixed layer [Lehmann *et al.*, 2005; B. G. Brunelle *et al.* Nitrate utilization and basin-shelf exchange in the upper water column of the Bering Sea, manuscript in preparation, 2007]. It is not clear how completely the surface nitrate pool is recharged during wintertime vertical mixing, but the supply of nitrate is dominated by wintertime processes, while the development of a strong salinity- and temperature-supported pycnocline suppresses mixing during the summer while improving the light conditions for phytoplankton growth [Gargett, 1991; Roden, 1995; Saitoh *et al.*, 2002; Harrison *et al.*, 2004]. There are a number of unique processes at work in the open Bering Sea, including dynamics associated with the “dicothermal layer” (the remnant base of the winter mixed layer) and exchange of water with the Alaskan shelf (B. G. Brunelle *et al.*, manuscript in preparation, 2007). Nevertheless, the system is relatively well characterized by an annual cycle of wintertime nitrate supply followed by summertime nitrate drawdown. Thus, for the

purposes of this manuscript, it is useful to discuss our results in the context of the Rayleigh model, in which a closed pool of substrate (nitrate) is progressively converted to organic N with a constant isotope effect [Mariotti *et al.*, 1981; Sigman *et al.*, 1999b] (the isotope effect being defined here as $(^{14}\text{k}/^{15}\text{k} - 1)$, where ^{14}k and ^{15}k are the rate coefficients for consumption of the ^{14}N - and ^{15}N -labeled forms of nitrate). If we consider $\delta^{15}\text{N}_{\text{db}}$ to track the $\delta^{15}\text{N}$ of the net organic matter production (i.e., the N exported from the surface), then there are three parameters that might explain the downcore changes we observe: (1) the $\delta^{15}\text{N}$ of the nitrate supply, (2) the isotope effect of nitrate assimilation, and (3) the fraction of gross nitrate supply that is consumed and transformed into exported N.

[32] Today, the $\delta^{15}\text{N}$ of nitrate feeding the mixed layer from below is $\sim 5.5\text{‰}$ [Lehmann *et al.*, 2005]. This is elevated slightly ($\sim 0.5\text{‰}$) above mean ocean nitrate because of denitrification in the North Pacific. During the LGM, in the eastern tropical Pacific and in the Arabian Sea, denitrification was reduced relative to interglacial conditions [Altabet *et al.*, 1995; Ganeshram *et al.*, 1995; Pride *et al.*, 1999; Emmer and Thunell, 2000; Ganeshram *et al.*, 2000; Kienast *et al.*, 2002; Galbraith *et al.*, 2004; Thunell and Kepple, 2004]. Thus one might have expected that the slight ^{15}N enrichment observed today would have been absent during glacial times, all else being equal. This $\sim 0.5\text{‰}$ effect, which in any case would cause the opposite sense of glacial/interglacial change from the observations, is too small to deserve more discussion. During the deglaciation, however, there is evidence for expansion of the eastern tropical Pacific denitrification zones, and the results of Cook *et al.* [2005] suggest that suboxia and accompanying denitrification existed within the Bering Sea at the same times that the eastern tropical North Pacific denitrification was most intense and/or expansive. Thus the effect of denitrification on the $\delta^{15}\text{N}$ of the nitrate supply dominates our thinking about the $\delta^{15}\text{N}$ variations in the deglacial section of JPC17 (see below).

[33] To explain the glacial/interglacial $\delta^{15}\text{N}$ difference by a change in the amplitude of the phytoplankton community's average isotope effect for nitrate assimilation would require a $\sim 3\text{‰}$ lower isotope effect during glacial times. Given that our estimate for the isotope effect in the modern Bering Sea is 4–6‰ (B. G. Brunelle *et al.*, manuscript in preparation, 2007), this would require a lower isotope effect in the glacial Bering Sea than has been measured anywhere in the modern ocean. Diatom species in the subarctic North Pacific change toward cold water, bloom-related species during glacial times [Sancetta, 1992; Katsuki *et al.*, 2003b; Katsuki and Takahashi, 2005], suggesting a reduced ice age role for the small nondiatom algae that are common in the modern open subarctic North Pacific and associated with iron limitation [Harrison *et al.*, 2004]. On the basis of the available culture data, a shift away from these small phytoplankton and toward large diatoms would, if anything, have led to a higher isotope effect during the last ice age [Montoya and McCarthy, 1995; Needoba *et al.*, 2003]. All else held constant, this would have lowered, not raised, the $\delta^{15}\text{N}$ of sinking N in the glacial Bering Sea. While Karsh *et al.* [2003] posed that iron fertilization during the Southern

Ocean Iron Enrichment Experiment (SOIREE) may have reduced the isotope effect for nitrate assimilation, we favor their alternative explanation that their observed $\delta^{15}\text{N}$ changes in suspended particles were the result of an increase in the nitrate-to-ammonium assimilation ratio of phytoplankton under iron enrichment [Price *et al.*, 1994; Timmermans *et al.*, 1998], which would not have an effect on the integrated sinking flux if ammonium is not exported from the mixed layer [Altabet, 1988].

[34] At the same time, we must recognize that diatom-bound N does not necessarily have a constant relationship with the integrated N flux out of the surface ocean. As described above, the community of diatoms and other phytoplankton growing in the Bering Sea may express different isotope effects for nitrate assimilation. If diatoms have a higher isotope effect than the other resident phytoplankton assimilators, this would work to lower their biomass $\delta^{15}\text{N}$ relative to the integrated N flux. If diatoms then became the only nitrate assimilators during glacial times, their $\delta^{15}\text{N}$ would, for a constant degree of nitrate utilization, increase as it converges toward the $\delta^{15}\text{N}$ of the sinking flux. Thus one might hypothesize that the glacial/interglacial change in $\delta^{15}\text{N}_{\text{db}}$ is due to a change in the relative importance of diatoms as nitrate assimilators. However, for diatom nitrate assimilation to increase as a fraction of total nitrate assimilation would require an increase in diatom production if one were to assume that nitrate utilization by the whole ecosystem and the gross nitrate supply rate held constant. This set of conditions seems to be violated by the observation of less diatom microfossil accumulation in glacial age sediments. Moreover, even in open ocean regions with iron limitation and a sizable population of nanoplankton and picoplankton, diatoms tend to be responsible for most of the nitrate assimilation [Harrison *et al.*, 2004], so a reduction in the relative quantity of nondiatom algae would not translate into a comparable change in the fraction of total nitrate assimilation attributable to diatoms.

[35] Thus the best explanation for the observed glacial/interglacial difference in $\delta^{15}\text{N}_{\text{db}}$ involves “nitrate utilization” [Altabet and Francois, 1994]: during glacial times, algal assimilation consumed a greater fraction of the gross nitrate supply to the Bering Sea surface. This led to a greater $^{15}\text{N}/^{14}\text{N}$ increase in the surface nitrate pool and an associated elevation in the $^{15}\text{N}/^{14}\text{N}$ of biomass produced from it. Given the $\sim 3\text{‰}$ amplitude of the glacial/interglacial $\delta^{15}\text{N}_{\text{db}}$ difference, an isotope effect for nitrate assimilation of $\sim 5\text{‰}$ in the Bering Sea (B. G. Brunelle *et al.*, manuscript in preparation, 2007), and roughly 50% nitrate consumption in the modern Bering Sea, the Rayleigh model estimates that the surface nitrate pool was nearly completely consumed during glacial times, a situation reminiscent of the modern Arctic. This calculation must be taken in the context of its many uncertainties, including the suitability of the Rayleigh model, but the data clearly call for a significant drop in the concentrations of the major nutrients.

[36] There are critical questions regarding diatom-bound organic N that will need to be addressed in culture and modern ocean studies. In particular, the Rayleigh model would predict that the $\delta^{15}\text{N}$ of sinking N in the modern

Bering Sea is $\sim 2\%$. This is $\sim 3\%$ lower than core top measurements of diatom-bound $\delta^{15}\text{N}$ in JPC17 (5–5.5‰). The magnitude of this offset between bulk sinking N and $\delta^{15}\text{N}_{\text{db}}$ is similar to that observed by *Robinson et al.* [2004] in the Antarctic. We have already addressed one possible explanation for this difference: diatoms may not express the same isotope effect as the entire nitrate-assimilating population of algae. However, as described above, the available culture data would tend to suggest a higher isotope effect for diatoms than other algae [*Montoya and McCarthy, 1995; Needoba et al., 2003*], which is in the opposite sense to explain the $\delta^{15}\text{N}$ difference between bulk sinking N and $\delta^{15}\text{N}_{\text{db}}$. An alternative explanation is that, of the N that diatoms assimilate, they tend to incorporate a ^{15}N -enriched fraction into diatom-bound organic matter. We are unable to assess the potential contribution of changes in this type of fractionation to the observed glacial/interglacial $\delta^{15}\text{N}_{\text{db}}$ change. We exclude them from our interpretation, but recognize that they will be critical to address in future work.

5.2. Upper Ocean Stratification During the Last Ice Age

[37] The diatom-bound N isotope data indicate that nitrate consumption was more complete during glacial times, when opal and Ba_{bio} both indicate that export production was lower than during interglacial conditions (Figure 3). As in studies reporting similar results from the Antarctic Zone of the Southern Ocean [*Francois et al., 1997; Sigman et al., 1999a; Robinson et al., 2004*], we conclude that this was the result of stronger upper ocean stratification during glacial times, which led to a lower gross flux of nitrate from the subsurface into the euphotic zone. Previous evidence from diatom and radiolarian assemblages have indeed argued for fresher, more stable, more Okhotsk-like conditions in the glacial Bering Sea, consistent with the stronger year-round stratification suggested by the N isotope data [*Morley and Hays, 1983; Sancetta, 1983; Sancetta et al., 1985; Katsuki and Takahashi, 2005; Tanaka and Takahashi, 2005*]. A consistent interpretation of glacial/interglacial change has been reported for the western open subarctic Pacific on the basis of a Ba_{bio} record from ODP Site 882 [*Jaccard et al., 2005*].

[38] As described in the introduction, nutrient consumption is incomplete in the Bering Sea today, most likely due to iron limitation [*Martin and Gordon, 1988; Tsuda et al., 2003*]. As the modern subarctic Pacific receives a significant fraction of its iron supply via aerial deposition (and possibly also by release from the shelves) [*Martin and Gordon, 1988; Fung et al., 2000*], less gross nutrient supply from the subsurface during the glacial would lead to a higher ratio of iron to major nutrients (a higher “ $\text{Fe}:\text{NO}_3^-$ ”) in the nutrient supply to the surface ocean. This makes the reasonable assumption that the atmospheric delivery of iron to the Bering Sea was not lower during the last ice age. In fact, it was likely higher, given the increased load of dust in the atmosphere [*Rohling et al., 2003*]. If iron is indeed the main limiting factor for algal growth in the subarctic Pacific [*Tsuda et al., 2003*], then the fraction of the major nutrient supply consumed in the surface would have been greater during glacial times. That export production was lower suggests that the total iron supply to the surface (that is, the

sum of the inputs from the subsurface and the atmosphere) was reduced during the last ice age; this would require that the supply of iron from the subsurface decreased more than the atmospheric supply increased. Alternatively, major nutrient consumption in the Bering might have proceeded essentially to completion. Finally, an additional mechanism for increasing nutrient consumption might be the benefit of increased light availability due to greater summertime stratification of the upper water column [*Haug et al., 2005*]. In general, this interpretation reconciles the geochemical evidence for reduced export production in the glacial subarctic Pacific with the diatom assemblage evidence for bloom-related diatom growth, in that these bloom-related diatom assemblages are today associated with iron inputs [*Sancetta, 1992; Katsuki et al., 2003b; Tsuda et al., 2003; Katsuki and Takahashi, 2005*].

5.3. Deglacial Changes

[39] While the large-scale glacial/interglacial changes in JPC17 seem well explained by the hypothesis of perennial stratification in the glacial subarctic Pacific, our picture of deglaciation is more complex and uncertain. The deglaciation is characterized by a transient switch from the inverse correlation between nutrient utilization and productivity that characterized the greater glacial/interglacial cycle to a largely positive correlation, suggesting that processes and/or conditions unique to the termination are influencing isotope and nutrient dynamics at our site.

5.3.1. Initial Deglacial $\delta^{15}\text{N}_{\text{db}}$ Decrease

[40] The initial decrease in benthic and planktonic $\delta^{18}\text{O}$ that marks the beginning of deglaciation is synchronous with a decrease in $\delta^{15}\text{N}_{\text{db}}$ (from 8.5‰ to 6.3‰; Figure 4). The $\delta^{15}\text{N}_{\text{db}}$ data are initially suggestive of a weakening in stratification at this time, possibly coincident with southern hemisphere changes, as would seem most consistent with the results of *Jaccard et al.* [2005]. However, the increase in export production that should have been associated with this breakdown in stratification is not apparent, given the low opal, biogenic barium, and CaCO_3 accumulation during this interval.

[41] One potential explanation is that if the upper water column remained stratified during the early deglaciation, but aerial Fe delivery to the surface declined [*Rohling et al., 2003*], then iron limitation may have effectively reduced the degree of macronutrient consumption without increasing productivity. Another possible explanation includes the formation of an extremely deep mixed layer upon deglaciation, leading to light limitation. While the former explanation is more plausible than the latter, neither is particularly convincing. In short, the apparent lack of increased production with the initial decrease in diatom $\delta^{15}\text{N}_{\text{db}}$ is not understood in the context of the glacial stratification hypothesis.

5.3.2. Deglacial $\delta^{15}\text{N}_{\text{db}}$ Peaks

[42] After 15.1 ka, $\delta^{15}\text{N}_{\text{db}}$ increases sharply from 6.3 to 8.5‰, coincident with the beginning of a green layer, marked by peaks in opal, CaCO_3 , and biogenic barium accumulation. A dramatic increase in export production has likewise been inferred in the open western subarctic Pacific and the Okhotsk Sea during the Bølling-Allerød [*Keigwin et*

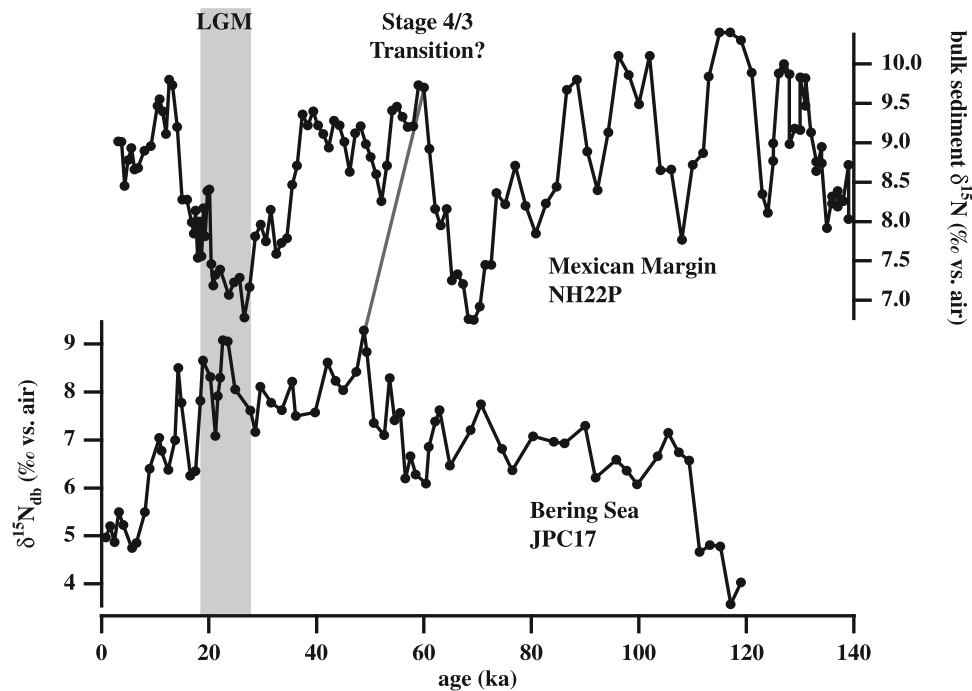


Figure 5. Comparison of $\delta^{15}\text{N}_{\text{db}}$ in JPC17 with a record of bulk sediment $\delta^{15}\text{N}$ from the Mexican margin (NH22P) extending back through stage 5 [Ganeshram *et al.*, 1995]. The age model for JPC17 from 0–49 ka is based on linear extrapolation between the available radiocarbon dates; beyond 49 ka, an accumulation rate of 12.4 cm/kyr (corresponding to the average accumulation rate for the radiocarbon-dated glacial period 20–42 ka) is applied to the remainder of the profile. The LGM is indicated by the shaded bar. The inferred stage 4/3 transition in JPC17 occurs too late given our age model (at 49 ka in JPC17 vs. at 60 ka in NH22P), which would require an overestimation of accumulation rate during this interval. The assignment of the stage 4/3 transition in JPC17 is supported by a slight increase in planktonic and benthic $\delta^{18}\text{O}$, but given the limited data, the assignment remains tentative.

al., 1992; Ternois *et al.*, 2001, Sato *et al.*, 2002, Seki *et al.*, 2004].

[43] Keigwin *et al.* [1992] suggested that nutrients released from melting ice and the potential benefits of enhanced light availability from a meltwater-induced stratification fostered the observed productivity increase in the open western subarctic Pacific. However, there are additional possible explanations for these two peaks in productivity. As mentioned previously, the two green layers in JPC17 correspond to laminated intervals in shallower cores from the Bering basin [Cook *et al.*, 2005]. The presence of these layers during the Bølling-Allerød and early Holocene suggests that suboxic to anoxic conditions prevailed throughout the middepths of the Bering Sea at these times [Cook *et al.*, 2005], which implies that the regenerated nutrient content of the subsurface was elevated. It is also possible that exposure of suboxic waters to the Bering Sea shelf would have increased the trace metal supply to surface waters.

[44] Depending on the cause for the deglacial peaks in productivity, $\delta^{15}\text{N}_{\text{db}}$ may have increased in part because of higher nitrate consumption associated with the increase in production [Nakatsuka *et al.*, 1995, Sigman *et al.*, 1993]. Nevertheless, it seems unavoidable that denitrification, in

the eastern North Pacific and/or in the Bering Sea itself, was responsible for at least part of the ^{15}N enrichment in the green layers. The suboxia within the Bering Sea indicated by the correlative laminated intervals in shallower cores from the Bering basin [Cook *et al.*, 2005] indicates that denitrification was active to some degree in the region, and the resulting $^{15}\text{N}/^{14}\text{N}$ increase in the subsurface nitrate would have been transported into the surface layer.

[45] The two-peak structure of $\delta^{15}\text{N}_{\text{db}}$ through the deglacial section is similar to the pattern observed throughout the eastern North Pacific (Figure 5) [Ganeshram *et al.*, 1995; Pride *et al.*, 1999; Emmer and Thunell, 2000; Kienast *et al.*, 2002] and in other regions through the deglaciation, when there was evidence of expansion in the tropical zones of thermocline suboxia that currently host denitrification [Zheng *et al.*, 2000; van Geen *et al.*, 2003]. On the one hand, given the similarity of the JPC17 record with the eastern North Pacific records, it is difficult to imagine that these lower latitude changes were not involved in generating the pattern of Bering Sea $\delta^{15}\text{N}_{\text{db}}$ change. On the other hand, denitrification is active today in the eastern tropical Pacific, yet the ^{15}N enrichment in the Bering Sea from exchange with that region is only $\sim 0.5\text{‰}$ [Lehmann *et al.*, 2005]. Thus the relative importance of local versus

regional denitrification in the deglacial $\delta^{15}\text{N}_{\text{db}}$ maxima is unclear. One view that subsumes the range of possibilities is that a circum-North Pacific decrease in middepth O_2 content upon the Bølling-Allerød warming expanded the eastern tropical zones of thermocline suboxia and pushed regions with relatively low bottom water O_2 (such as the middepth Bering Sea, currently with $\sim 15 \mu\text{M} [\text{O}_2]$ [Roden, 1995]) into suboxia, leading to widespread water column denitrification.

[46] When inspected in detail, the inferred stage 4/3 transition in JPC17 has many similarities with the transition from the LGM to the Holocene, with the former appearing to be a muted version of the latter (Figure 3). Immediately following the first sign of cooling in the $\delta^{18}\text{O}$ record, marking the onset of stage 4, $\delta^{15}\text{N}_{\text{db}}$ rises and reaches values higher than any previously reached in stage 5, while opal decreases from ~ 60 to $\sim 20\%$ (at ~ 725 cm). It thus appears that cooling has led to enhanced stratification, and therefore higher degrees of nutrient utilization and lower productivity, as is observed in the LGM. After this interval, $\delta^{15}\text{N}_{\text{db}}$ decreases slightly (689–713 cm), accompanied by mild increases in opal content and Ba_{bio} . Finally, at the inferred onset of stage 3 (at ~ 672 cm), $\delta^{15}\text{N}_{\text{db}}$ rises sharply again, with opal and Ba_{bio} increasing as well, mimicking, on a muted scale, the events of the last deglaciation. Given the lack of evidence for Bering Sea lamination during this period (M. Cook, unpublished data, 2003), the moderate rise in $\delta^{15}\text{N}_{\text{db}}$ at the commencement of stage 3 would be best explained by an increase in the $\delta^{15}\text{N}$ of nitrate derived from the low-latitude thermocline, which resumes denitrification at this time [Ganeshram et al., 1995; Kienast et al., 2002].

5.4. Comparison of Bulk Sediment $\delta^{15}\text{N}$ and Diatom-Bound $\delta^{15}\text{N}$

[47] During full interglacial conditions, bulk sediment $\delta^{15}\text{N}$ and $\delta^{15}\text{N}_{\text{db}}$ are roughly equivalent at 5.0–5.5‰. As described above, surface nitrate in the modern Bering Sea suggests a $\delta^{15}\text{N}$ of $\sim 2\%$ for the annually integrated sinking flux. It appears then that diagenetic alteration has raised Holocene bulk sediment $\delta^{15}\text{N}$ by about 3‰, which is typical of the effect observed in previous studies of nonmargin sites [Altabet and Francois, 1994; Altabet et al., 1999]. The high Holocene sedimentation rate (of ~ 15 cm/kyr) may raise the question of whether a diagenetic offset would be expected at JPC17, given the evidence for minimal diagenetic offsets in margin sediments from highly productive settings [e.g., Altabet et al., 1999]. However, the organic carbon content of the near-surface sediments (~ 0.7 wt %) suggests that the extent of organic matter degradation is indeed typical of offshore sediments [Hedges et al., 1999]. The $\delta^{15}\text{N}_{\text{db}}$ is also higher than the calculated value for the integrated sinking flux, presumably due to internal fractionation within the diatom, as discussed above.

[48] Under glacial conditions, however, $\delta^{15}\text{N}_{\text{db}}$ is higher than bulk sediment $\delta^{15}\text{N}$ by $\sim 2\%$. A glacial age increase in the efficiency of the global ocean biological pump by reduced overturning and CO_2 outgassing in the polar ocean (i.e., the Antarctic stratification hypothesis [Francois et al., 1997; Sigman and Boyle, 2000]) would lower the O_2

content of the deep ocean [Knox and McElroy, 1984; Sarmiento and Toggweiler, 1984; Siegenthaler and Wenk, 1984]. Under these conditions, the isotopic alteration of sedimentary N may have been reduced [Altabet et al., 1999; Thunell et al., 2004] either because of less complete remineralization of sedimentary organic matter or a different isotopic impact of remineralization under suboxic conditions [Lehmann et al., 2004]. Thus we propose that the change in the relationship between bulk sedimentary and diatom-bound $\delta^{15}\text{N}$ is due to a $\sim 2\%$ reduction in the diagenetic ^{15}N enrichment of bulk sedimentary N under lower O_2 glacial conditions. Even if this hypothesis is correct, it is unclear whether stratification in the subarctic Pacific played any role in the deep O_2 change, or whether this change was driven entirely from the Southern Ocean (see Jaccard et al. [2005] for a related discussion regarding dissolved inorganic carbon and calcite saturation state).

6. Discussion

6.1. Physical Mechanism for Bering Sea Stratification During the Last Ice Age

[49] Given the previous work in the North Pacific and in the Antarctic Zone of the Southern Ocean, physical mechanisms linking cold climates to polar ocean stratification have already been considered. We discuss these in the context of the Bering Sea.

[50] As the Bering Strait allows the escape of fresh water from the modern subarctic Pacific, the absence of the strait during glacial times may work to strengthen the halocline. While this process may contribute to our observations, the opening of the strait appears to occur too late (at ~ 13 ka) to explain the inferred deglacial changes in stratification [Elias et al., 1997]. Moreover, it cannot explain the evidence from the open subarctic Pacific for a tight connection with southern hemisphere changes [Jaccard et al., 2005].

[51] Sea ice melting is an obvious mechanism for producing local stratification. One would tend to expect a more active sea ice cycle in the subarctic Pacific during the last ice age, and winter sea ice extent in the Bering Sea was indeed greater during the last ice age (Figure 1) [Sancetta, 1983; Sancetta et al., 1985; Katsuki et al., 2003a; Katsuki and Takahashi, 2005]. Evidence for a better ventilated intermediate-depth water mass in the North Pacific during the LGM also suggests that sea ice formation and brine rejection processes continued during this time, potentially at greater rates than today [Duplessy et al., 1988; Keigwin, 1998]. The transport of this ice into the open Bering Sea, followed by melting, would have likely worked to stratify that region.

[52] However, we hesitate to suggest that a more rigorous sea ice cycle alone can explain the inferred reduction in surface nutrients. Since brine ejected from forming sea ice is efficiently entrained in the mixed layer, sea ice formation drives densification of the mixed layer and thus promotes overturning where it occurs. If more vigorous overturning occurred at the northern slope of the Bering Sea (with the modern shelves above sea level during the LGM), it would import nutrients into the upper ocean, which would then be transported across the Bering Sea by the upper ocean

circulation. The melting of ice during the summer would indeed stabilize the water column; however, this change would apply to a season of minimal nutrient entrainment in the modern Bering Sea. Thus it seems unlikely that sea ice melting would in fact reduce the gross upward transport of nitrate that we infer for the glacial Bering Sea. Moreover, the production and melting of sea ice are local processes that would be expected to affect productivity differently and to varying degrees among regions. Yet a number of records from the subarctic Pacific as well as the Antarctic all suggest that stratification was stronger [Morley and Hays, 1983; Sancetta, 1983; Sancetta et al., 1985; Francois et al., 1997; Narita et al., 2002; Jaccard et al., 2005; Katsuki and Takahashi, 2005; Okazaki et al., 2005a, 2005b; Tanaka and Takahashi, 2005] and productivity lower during the LGM [Mortlock et al., 1991; Kumar et al., 1995; Gorbarenko, 1996; Sato et al., 2002; Nürnberg and Tiedemann, 2004]. A more global mechanism may thus be necessary to explain the similarity of productivity changes observed over large expanses of the polar oceans.

[53] An equatorward shift and weakening in the westerly winds has been proposed to explain evidence for Antarctic stratification during the last ice age [Toggweiler et al., 2006]. One can imagine that a hemispherically symmetric situation in the subarctic Pacific might apply, with the northern hemisphere westerly winds migrating southward and weakening under colder climates, driving less intense divergence. This mechanism may work less well for the subarctic Pacific than it does in the Southern Ocean. In particular, the open channel that is central to the role of winds in driving deep water upwelling in the Southern Ocean [Toggweiler and Samuels, 1995] is lacking in the North Pacific, so there is no dynamical constraint against lower latitude surface waters replacing the subarctic Pacific surface water that is lost to the south by Ekman transport. Nevertheless, Ekman divergence clearly causes shoaling of isopycnals in the modern subarctic Pacific, so this mechanism cannot be ruled out. It is also possible that overturning and stratification in the subarctic Pacific can be driven remotely by the southern hemisphere westerlies, so as to drive synchronous and similar changes in the Antarctic and subarctic Pacific (A. M. de Boer et al., Atlantic dominance of the Meridional Overturning Circulation, submitted to *Journal of Physical Oceanography*, 2007).

[54] A mechanism that would work to drive bihemispheric polar ocean stratification during cold climates involves the reduced sensitivity of seawater density to temperature at low mean ocean temperatures [Winton, 1997; Wang et al., 2002; Sigman et al., 2004; de Boer et al., 2007]. Polar ocean regions, the subarctic Pacific and Antarctic in particular, are pushed toward overturning by temperature, with cooling at the top during the winter, and toward stratification by salinity, with freshwater added to the top from the lower latitudes through the hydrological cycle. Homogenous cooling of the polar ocean water column weakens the role of temperature so as to reduce its opposition to the stratifying effects of salinity [Sigman et al., 2004]. In net, homogenous cooling can thus drive polar ocean stratification. In experiments with an ocean general circulation model, this effect is found to be of first order for

both the Antarctic and North Pacific, where the salinity stratification is strong [de Boer et al., 2007]. According to this mechanism, deglacial overturning would be paced by deep ocean warming. Given the different times of deglacial response from $\delta^{15}\text{N}_{\text{db}}$ and the productivity proxies (the first beginning at 17.5 ka but the latter near the beginning of the Bølling-Allerød at 15.1 ka), it remains unclear when Bering Sea stratification weakened. With increased information on the timing of the upper ocean changes in the subarctic North Pacific and on deep North Pacific temperature change [Skinner and Shackleton, 2005], it should be possible to evaluate their consistency with the temperature/stratification mechanism.

6.2. Link Between Bering Sea Nutrient Status and Eastern Pacific Denitrification

[55] The nutrient content of newly formed mode and intermediate water masses (i.e., their “preformed” nutrient content) influences the amount of productivity, nutrient trapping, and oxygen consumption that occurs in lower latitude regions of upwelling [Toggweiler and Carson, 1995; Sigman et al., 2003; Sarmiento et al., 2004]. On this basis, it has been posed that the glacial reduction in middepth nutrient content, suboxia, and denitrification in the Pacific was driven or encouraged by enhanced nutrient drawdown in the regions of Subantarctic Mode Water formation in the Southern Ocean [Robinson et al., 2005]. The thermocline of the eastern tropical North Pacific is partially ventilated by intermediate waters formed in the subarctic Pacific. Thus we might expect to observe an inverse relationship between nutrient utilization in the subarctic Pacific and suboxia and denitrification in the eastern tropical North Pacific. Indeed, during glacial times, when nutrient utilization was apparently greater in the Bering Sea, the presence of bioturbated sediment and low bulk sediment $\delta^{15}\text{N}$ in the eastern tropical North Pacific indicate reduced suboxia and water column denitrification (Figure 5) [Ganeshram et al., 1995]. Although nutrient delivery from the high latitudes is not the only control on low-latitude water column denitrification, the coincidence of glacial-to-interglacial changes in high-latitude nutrient utilization and low-latitude denitrification argue for a link between these processes. Moreover, as described above, the inferred stage 4/3 transition is interestingly similar to the glacial termination in terms of $\delta^{15}\text{N}_{\text{db}}$ changes and their connections to $\delta^{15}\text{N}$ changes in the ETNP (section 5.3), again suggesting a link between polar ocean nutrient status and tropical thermocline suboxia.

[56] However, the detailed timing of the glacial-to-interglacial decrease in Bering Sea nitrate utilization relative to the lower latitude denitrification increase will need to be resolved before we will have a sense of how important this forcing was relative to others that have been proposed [Keigwin and Jones, 1990; Kennett and Ingram, 1995; Behl and Kennett, 1996; van Geen et al., 1996; Keigwin, 1998; Galbraith et al., 2004; Meissner et al., 2005], with regard to both the basic glacial-to-interglacial increase in eastern North Pacific denitrification and its deglacial peaks. Upon the initial decrease in benthic $\delta^{18}\text{O}$ in JPC17 at ~ 17.5 ka, $\delta^{15}\text{N}_{\text{db}}$ in the Bering Sea decreases, which may

be synchronous with a small initial rise in bulk sediment $\delta^{15}\text{N}$ observed in cores from the Mexican margin, the Santa Barbara Basin, and off the coast of Oregon (Figure 5) [Ganeshram *et al.*, 1995; Emmer and Thunell, 2000; Kienast *et al.*, 2002]. However, in at least some eastern North Pacific records, the sharpest $\delta^{15}\text{N}$ increase occurs at the onset of Bølling-Allerød warming at ~ 14.5 ka (Figure 5). Because deglacial denitrification signals also exist in the Bering Sea during these times, we cannot easily reconstruct how subarctic Pacific nutrient utilization changed through this time interval. Finally, there are aspects of the eastern North Pacific denitrification changes that our Bering Sea data clearly cannot explain. In particular, suboxia and denitrification appear to wane subsequent to deglaciation [Pride *et al.*, 1999; Zheng *et al.*, 2000], whereas Bering Sea nutrient utilization does not clearly increase through early to mid-Holocene. The apparent Holocene weakening in eastern North Pacific denitrification may be an internal response to the climate-forced deglacial denitrification increase [Deutsch *et al.*, 2004] or may indicate that the deglacial peaks in suboxia and denitrification have a cause specifically associated with the unique transient conditions of the deglaciation (see below).

[57] While we have proposed above an overarching modulation of ETNP suboxia by the nutrient status of the subarctic Pacific, we doubt that this process is responsible for the transient deglacial (Bølling-Allerød and early Holocene) $\delta^{15}\text{N}$ peaks in the Bering Sea itself (Figure 5). Though a deglacial decrease in nutrient utilization in the Bering Sea may work to increase suboxia in the ETNP, it would tend to reduce suboxia in its own middepth waters. Increased productivity during the deposition of the green layers has been considered as a cause for the Bering Sea suboxia [Cook *et al.*, 2005]. However, this will depend on the circulation changes driving that production increase. Given the occurrence of the Bering Sea laminations during deglacial warming and sea level rise (e.g., the Bølling-Allerød) [Fairbanks, 1989], it seems plausible that melting ice sheets worked to stratify the upper water column of the Bering Sea and encouraged middepth suboxia by reducing North Pacific Intermediate Water formation [Cook *et al.*, 2005]. Given the similarity of the deglacial events in the Bering Sea and ETNP, such polar forcing might also have reduced thermocline ventilation so as to explain the deglacial $\delta^{15}\text{N}$ peaks in the ETNP [Meissner *et al.*, 2005].

7. Summary and Perspective

[58] Polar ocean overturning is important for the exchange of CO_2 between the ocean and atmosphere in the contexts of both glacial/interglacial cycles [Toggweiler, 1999; Sigman and Boyle, 2000] and anthropogenic CO_2 inputs [Sarmiento *et al.*, 1998]. Comparison of the responses of different polar ocean regions to glacial/interglacial cycles may allow for a fundamental understanding of their climate sensitivities and impacts.

[59] In JPC17 from the central Bering basin, sediments from the last glacial period have high diatom-bound $\delta^{15}\text{N}$ coupled with low concentrations of biogenic barium and opal, suggesting that the gross nitrate supply to the surface

ocean was more completely consumed during glacial times even though algal productivity was lower. This set of observations, analogous to previous results from the Antarctic [Francois *et al.*, 1997; Sigman *et al.*, 1999a; Robinson *et al.*, 2004], suggests that the Bering Sea and the subarctic Pacific in general was more strongly stratified during the last ice age. This study thus appears to confirm earlier hypotheses [Narita *et al.*, 2002; Jaccard *et al.*, 2005] and strengthens the case for a pervasive link between cold climates and stratification of the halocline-bearing polar ocean regions.

[60] Moreover, the present study illuminates the similarities and differences between the subarctic Pacific and the Antarctic of the Southern Ocean. In particular, that nitrate utilization in the Bering Sea is persistently higher under ice age stratification is consistent with the evidence that the subarctic Pacific gets a significant fraction of its iron supply from the atmosphere, which will continue to provide this critical trace nutrient even as the supply of all nutrients (the major and trace nutrients) decreases with reduced vertical exchange between surface and subsurface. In the Antarctic, higher nitrate consumption may not be as pervasive during the last ice age [Robinson *et al.*, 2004], perhaps due to a limited role for atmospheric iron inputs in this region [Lefevre and Watson, 1999; Archer and Johnson, 2000].

[61] The evidence for a deglacial increase in suboxia and water column denitrification is the dominant signal of bulk sediment $^{15}\text{N}/^{14}\text{N}$ records from the eastern tropical Pacific. We propose above that higher nutrient utilization in the subarctic Pacific reduced the preformed nutrient concentration of glacial age North Pacific Intermediate Water and thereby worked to reduce the extent of suboxia and denitrification in the thermocline of the eastern North Pacific. A detailed study of the timing and nature of the deglacial decline in nitrate utilization in the subarctic Pacific relative to the lower latitude denitrification increase will provide an important test of this hypothesis. However, even with higher temporal resolution studies of the subarctic Pacific, one will still be faced with the interfering N isotope signals of nitrate utilization and denitrification.

[62] Deglacial peaks in diatom-bound and bulk sedimentary $\delta^{15}\text{N}$ in JPC17 occur within “green layers” that correlate with periods of suboxia in the middepth Bering Sea and that at least partially result from denitrification, within the Bering Sea and/or in the eastern tropical North Pacific. To this point, paleoceanographic N isotope studies of high-latitude sediment cores have tended to focus on the nutrient status of the surface waters, while low-latitude studies have focused on fixed N inputs and outputs (i.e., N_2 fixation and denitrification). These tendencies are clearly sensible, especially for the early stages of the field. However, this and other recent studies are making clear that a strict separation of these subjects is not realistic. First, polar ocean regions greatly affect the physical and biogeochemical conditions of the low latitudes, largely through thermocline ventilation [Galbraith *et al.*, 2004; Sarmiento *et al.*, 2004; Robinson *et al.*, 2005]. Second, low-latitude processes (such as denitrification in the major low-latitude suboxic zones) can drive regional and global signals in the isotopic composition of subsurface nitrate, which are

then sampled by the polar ocean surface [Sigman *et al.*, 2000; Deutsch *et al.*, 2004; Lehmann *et al.*, 2005]. Overcoming this complexity and turning it to our advantage should be a central goal for paleoceanographic studies using the N isotopes.

[63] **Acknowledgments.** This manuscript greatly benefited from a review by Bob Anderson, as well as discussions with Michael Bender and Rebecca Robinson. Financial support for this work was provided by NSF grants OCE-0136449, OCE-9981479, ANT-0453680, by BP and Ford Motor Company through the Princeton Carbon Migration Initiative, and by a NDEG fellowship to B.G.B. Work conducted aboard the USCG *Healy* (Healy 0202) was funded by grant OPP-9912122.

References

- Altabet, M. (1988), Variations in nitrogen isotopic composition between sinking and suspended particles—Implications for nitrogen cycling and particle transformation in the open ocean, *Deep Sea Res., Part A*, 35(4), 535–554.
- Altabet, M. A. (1996), Nitrogen and carbon isotope tracers of the source and transformation of particles in the deep-sea, in *Particle Flux in the Ocean*, edited by V. Ittekkot *et al.*, pp. 155–184, John Wiley, Hoboken, N. J.
- Altabet, M. A., and R. Francois (1994), Sedimentary nitrogen isotopic ratio as a recorder for surface ocean nutrient utilization, *Global Biogeochem. Cycles*, 8, 103–116.
- Altabet, M. A., and R. Francois (2001), Nitrogen isotope biogeochemistry of the Antarctic polar frontal zone at 170°W, *Deep Sea Res., Part II*, 48, 4247–4273.
- Altabet, M. A., R. Francois, D. W. Murray, and D. W. Prell (1995), Climate-related variations in denitrification in the Arabian Sea from sediment ¹⁵N/¹⁴N ratios, *Nature*, 373(6514), 506–509.
- Altabet, M. A., C. Pilskaln, R. Thunell, C. Pride, D. Sigman, F. Chavez, and R. Francois (1999), The nitrogen isotope biogeochemistry of sinking particles from the margin of the eastern North Pacific, *Deep Sea Res., Part I*, 46, 655–679.
- Anderson, R. F., Z. Chase, M. Q. Fleisher, and J. Sachs (2002), The Southern Ocean's biological pump during the Last Glacial Maximum, *Deep Sea Res., Part II*, 49, 1909–1938.
- Archer, D. E., and K. Johnson (2000), A model of the iron cycle in the ocean, *Global Biogeochem. Cycles*, 14, 269–279.
- Barford, C. C., J. P. Montoya, M. A. Altabet, and R. Mitchell (1999), Steady-state nitrogen isotope effects of N₂ and N₂O production in *Paracoccus denitrificans*, *Appl. Environ. Microbiol.*, 65(3), 989–994.
- Behl, R. J., and J. P. Kennett (1996), Brief interstadial events in the Santa Barbara Basin, NE Pacific, during the past 60 kyr, *Nature*, 379(6562), 243–246.
- Braman, R. S., and S. A. Hendrix (1989), Nanogram nitrite and nitrate determination in environmental and biological materials by vanadium (iii) reduction with chemi-luminescence detection, *Anal. Chem.*, 61(24), 2715–2718.
- Casciotti, K. L., D. M. Sigman, M. G. Hastings, J. K. Bohlke, and A. Hilkert (2002), Measurement of the oxygen isotopic composition of nitrate in seawater and freshwater using the denitrifier method, *Anal. Chem.*, 74(19), 4905–4912.
- Choi, M. S., R. Francois, K. Sims, M. P. Bacon, S. Brown-Leger, A. P. Fleer, L. Ball, D. Schneider, and S. Pichat (2001), Rapid determination of Th-230 and Pa-231 in seawater by desolvated micro-nebulization inductively coupled plasma magnetic sector mass spectrometry, *Mar. Chem.*, 76(1–2), 99–112.
- Cline, J. D., and I. R. Kaplan (1975), Isotopic fractionation of dissolved nitrate during denitrification in the eastern tropical North Pacific Ocean, *Mar. Chem.*, 3(4), 271–299.
- Codispoti, L. A., J. A. Brandes, J. P. Christensen, A. H. Devol, S. W. A. Naqvi, H. W. Pearl, and T. Yoshinari (2001), The ocean fixed nitrogen and nitrous oxide budgets: Moving targets as we enter the anthropocene?, *Sci. Mar.*, 65, 85–105.
- Cook, M. S., L. D. Keigwin, and C. A. Sancetta (2005), The deglacial history of surface and intermediate water of the Bering Sea, *Deep Sea Res., Part II*, 52, 2163–2173.
- Crosta, X., and A. Shemesh (2002), Reconciling down core anticorrelation of diatom carbon and nitrogen isotopic ratios from the Southern Ocean, *Paleoceanography*, 17(1), 1010, doi:10.1029/2000PA000565.
- Crosta, X., A. Shemesh, M. E. Salvignac, H. Gildor, and R. Yam (2002), Late Quaternary variations of elemental ratios (C/Si and N/Si) in diatom-bound organic matter from the Southern Ocean, *Deep Sea Res., Part II*, 49, 1939–1952.
- Crusius, J., T. F. Pedersen, S. Kienast, L. Keigwin, and L. Labeyrie (2004), Influence of northwest Pacific productivity on North Pacific Intermediate Water oxygen concentrations during the Bolling-Allerod interval (14.7–12.9 ka), *Geology*, 32(7), 633–636.
- de Boer, A. M., D. M. Sigman, and J. R. Toggweiler (2007), The effect of global ocean temperature change on deep ocean ventilation, *Paleoceanography*, doi:10.1029/2005PA001242, in press.
- Deutsch, C., D. M. Sigman, R. C. Thunell, A. N. Meckler, and G. H. Haug (2004), Isotopic constraints on glacial/interglacial changes in the oceanic nitrogen budget, *Global Biogeochem. Cycles*, 18, GB4012, doi:10.1029/2003GB002189.
- Duplessy, J. C., N. J. Shackleton, R. G. Fairbanks, L. Labeyrie, D. Oppo, and N. Kallel (1988), Deepwater source variations during the last climatic cycle and their impact on the global deepwater circulation, *Paleoceanography*, 3, 343–360.
- Dymond, J., E. Suess, and M. Lyle (1992), Barium in deep-sea sediment: A geochemical proxy for paleoproductivity, *Paleoceanography*, 7, 163–181.
- Elderfield, H., and R. E. M. Rickaby (2000), Oceanic Cd/P ratio and nutrient utilization in the glacial Southern Ocean, *Nature*, 405(6784), 305–310.
- Elias, S. A., S. K. Short, and H. H. Birks (1997), Late Wisconsinan environments of the Bering Land Bridge, *Paleogeogr. Paleoclimatol. Paleoecol.*, 136, 293–308.
- Emmer, E., and R. C. Thunell (2000), Nitrogen isotope variations in Santa Barbara Basin sediments: Implications for denitrification in the eastern tropical North Pacific during the last 50,000 years, *Paleoceanography*, 15, 377–387.
- Fairbanks, R. G. (1989), A 17,000-year glacio-eustatic sea-level record—Influence of glacial melting rates on the Younger Dryas event and deep-ocean circulation, *Nature*, 342(6250), 637–642.
- Farrell, J. W., T. F. Pedersen, S. E. Calvert, and B. Nielsen (1995), Glacial-interglacial changes in nutrient utilization in the equatorial Pacific Ocean, *Nature*, 377(6549), 514–517.
- Francois, R., M. A. Altabet, E.-F. Yu, D. M. Sigman, M. P. Bacon, M. Frank, G. Bohrmann, G. Bareille, and L. D. Labeyrie (1997), Contributions of Southern Ocean surface-water stratification to low atmospheric CO₂ concentrations during the last glacial period, *Nature*, 389(6654), 929–935.
- Francois, R., M. Frank, M. M. Rutgers van der Loeff, and M. P. Bacon (2004), ²³⁰Th normalization: An essential tool for interpreting sedimentary fluxes during the late Quaternary, *Paleoceanography*, 19, PA1018, doi:10.1029/2003PA000939.
- Fung, I. Y., S. K. Meyn, I. Tegen, S. C. Doney, J. G. John, and J. K. B. Bishop (2000), Iron supply and demand in the upper ocean, *Global Biogeochem. Cycles*, 14, 281–295.
- Galbraith, E. D., M. Kienast, T. F. Pedersen, and S. E. Calvert (2004), Glacial-interglacial modulation of the marine nitrogen cycle by high-latitude O₂ supply to the global thermocline, *Paleoceanography*, 19, PA4007, doi:10.1029/2003PA001000.
- Ganeshram, R. S., T. F. Pedersen, S. E. Calvert, and J. W. Murray (1995), Large changes in ocean nutrient inventories from glacial to interglacial periods, *Nature*, 376(6543), 755–758.
- Ganeshram, R. S., T. F. Pedersen, S. E. Calvert, G. W. McNeill, and M. R. Fontugne (2000), Glacial-interglacial variability in denitrification in the world's oceans: Causes and consequences, *Paleoceanography*, 15, 361–376.
- Gargett, A. E. (1991), Physical processes and the maintenance of nutrient-rich euphotic zones, *Limnol. Oceanogr.*, 36(8), 1527–1545.
- Gorbarenko, S. A. (1996), Stable isotope and lithologic evidence of late-glacial and Holocene oceanography of the northwestern Pacific and its marginal seas, *Quat. Res.*, 46(3), 230–250.
- Harrison, P. J., F. A. Whitney, A. Tsuda, H. Saito, and K. Tadokoro (2004), Nutrient and plankton dynamics in the NE and NW gyres of the subarctic Pacific Ocean, *J. Oceanogr.*, 60(1), 93–117.
- Haug, G. H., *et al.* (2005), North Pacific seasonality and the glaciation of North America 2.7 million years ago, *Nature*, 433(7028), 821–825.
- Hedges, J. I., F. S. Hu, A. H. Devol, H. E. Hartnett, E. Tsamakis, and R. G. Keil (1999), Sedimentary organic matter preservation: A test for

- selective degradation under oxic conditions, *Am. J. Sci.*, 299, 529–555.
- Hendersen, G. M. and R. F. Anderson (2003), The U-series toolbox for paleoceanography, in *U-Series Geochemistry*, *Rev. Mineral. Geochem.*, vol. 52, edited by B. Bourdon et al., pp. 493–531, Mineral. Soc. of Am., Washington, D. C.
- Hughen, K., S. Lehman, J. Southon, J. Overpeck, O. Marchal, C. Herring, and J. Turnbull (2004), ^{14}C activity and global carbon cycle changes over the past 50,000 years, *Science*, 303(5655), 202–207.
- Ingalls, A. E., C. Lee, S. G. Wakeham, and J. I. Hedges (2003), The role of biominerals in the sinking flux and preservation of amino acids in the Southern Ocean along 170°W , *Deep Sea Res.*, Part II, 50, 713–738.
- Ingalls, A. E., R. F. Anderson, and A. Pearson (2004), Radiocarbon dating of diatom-bound organic compounds, *Mar. Chem.*, 92(1–4), 91–105.
- Jaccard, S. L., G. H. Haug, D. M. Sigman, T. F. Pedersen, H. R. Thierstein, and U. Rohl (2005), Glacial/interglacial changes in subarctic North Pacific stratification, *Science*, 308(5724), 1003–1006.
- Karsh, K. L., T. W. Trull, A. J. Lourey, and D. M. Sigman (2003), Relationship of nitrogen isotope fractionation to phytoplankton size and iron availability during the Southern Ocean Iron Release Experiment (SOIREE), *Limnol. Oceanogr.*, 48(3), 1058–1068.
- Katsuki, K., and K. Takahashi (2005), Diatoms as paleoenvironmental proxies for seasonal productivity, sea-ice and surface circulation in the Bering Sea during the late Quaternary, *Deep Sea Res.*, Part II, 52, 2110–2130.
- Katsuki, K., K. Takahashi, R. W. Jordan, K. Matsushita, and T. Sengoku (2003a), Surface circulation changes based on fossil diatoms in the Bering Sea and western subarctic Pacific, *Kaiyo Mon.*, 35, 394–400.
- Katsuki, K., K. Takahashi, and M. Okada (2003b), Diatom assemblage and productivity changes during the last 340,000 years in the subarctic Pacific, *J. Oceanogr.*, 59(5), 695–707.
- Keigwin, L. D. (1998), Glacial-age hydrography of the far northwest Pacific Ocean, *Paleoceanography*, 13, 323–339.
- Keigwin, L. D., and G. A. Jones (1990), Deglacial climatic oscillations in the Gulf of California, *Paleoceanography*, 5, 1009–1023.
- Keigwin, L. D., G. A. Jones, and P. N. Froelich (1992), A 15,000 year paleoenvironmental record from Meji Seamount far northwestern Pacific, *Earth Planet. Sci. Lett.*, 111(2–4), 425–440.
- Kennett, J. P., and B. L. Ingram (1995), A 20,000-year record of ocean circulation and climate change from the Santa Barbara basin, *Nature*, 377(6549), 510–514.
- Kienast, S. S., S. E. Calvert, and T. F. Pedersen (2002), Nitrogen isotope and productivity variations along the northeast Pacific margin over the last 120 kyr: Surface and subsurface paleoceanography, *Paleoceanography*, 17(4), 1055, doi:10.1029/2001PA000650.
- Kienast, S. S., I. L. Hendy, J. Crusius, T. F. Pedersen, and S. E. Calvert (2004), Export Production in the Subarctic North Pacific over the last 800 kyr: No evidence for iron fertilization?, *J. Oceanogr.*, 60(1), 189–203.
- King, K. (1977), Amino acid survey of recent calcareous and siliceous deep-sea microfossils, *Micropaleontology*, 23, 180–193.
- Knapp, A. N., and D. M. Sigman (2003), Stable isotopic composition of dissolved organic nitrogen from the surface waters of the Sargasso Sea, paper presented at ASLO Annual Meeting, Salt Lake City, Utah.
- Knox, F., and M. McElroy (1984), Changes in atmospheric CO_2 influence of the marine biota at high latitude, *J. Geophys. Res.*, 89, 4629–4637.
- Kröger, N., R. Deutzmann, C. Bergsdorf, and M. Sumper (2000), Species-specific polyamines from diatoms control silica morphology, *Proc. Natl. Acad. Sci. U.S.A.*, 97(26), 14,133–14,138.
- Kumar, N., R. F. Anderson, R. A. Mortlock, P. N. Froelich, P. Kubik, B. Ditttrich-Hannen, and M. Suter (1995), Increased biological productivity and export production in the glacial Southern Ocean, *Nature*, 378(6558), 675–680.
- Lefevre, N., and A. J. Watson (1999), Modeling the geochemical cycle of iron in the oceans and its impact on atmospheric CO_2 concentrations, *Global Biogeochem. Cycles*, 13, 727–736.
- Lehmann, M. F., S. M. Bernasconi, J. A. McKenzie, A. Barbieri, M. Simona, and M. Veronesi (2004), Seasonal variation of the $\delta^{13}\text{C}$ and $\delta^{15}\text{N}$ of particulate and dissolved carbon and nitrogen in Lake Lugano: Constraints on biogeochemical cycling in a eutrophic lake, *Limnol. Oceanogr.*, 49(2), 415–429.
- Lehmann, M. F., D. M. Sigman, D. C. McCorkle, B. G. Brunelle, S. Hoffmann, M. Kienast, G. Cane, and J. Clement (2005), Origin of the deep Bering Sea nitrate deficit: Constraints from the nitrogen and oxygen isotopic composition of water column nitrate and benthic nitrate fluxes, *Global Biogeochem. Cycles*, 19, GB4005, doi:10.1029/2005GB002508.
- Liu, K. K., and I. R. Kaplan (1989), The eastern tropical Pacific as a source of ^{15}N -enriched nitrate in seawater off southern California, *Limnol. Oceanogr.*, 34(5), 820–830.
- Lourey, M. J., T. W. Trull, and D. M. Sigman (2003), Sensitivity of $\delta^{15}\text{N}$ of nitrate, surface suspended and deep sinking particulate nitrogen to seasonal nitrate depletion in the Southern Ocean, *Global Biogeochem. Cycles*, 17(3), 1081, doi:10.1029/2002GB001973.
- Mariotti, A., G. C. Germon, P. Hubert, P. Kaiser, R. Létolle, A. Tardieux, and P. Tardieux (1981), Experimental determination of nitrogen kinetic isotope fractionation: Some principles: Illustrations for the denitrification and nitrification processes, *Plant Soil*, 62, 413–430.
- Martin, J. H., and R. M. Gordon (1988), Northeast Pacific iron distributions in relation to phytoplankton productivity, *Deep Sea Res.*, 35, 177–196.
- Martin, J. H., S. E. Fitzwater, and R. M. Gordon (1990), Iron deficiency limits growth in Antarctic waters, *Global Biogeochem. Cycles*, 4, 5–12.
- McManus, J., et al. (1998), Geochemistry of barium in marine sediments: Implications for its use as a paleoproxy, *Geochim. Cosmochim. Acta*, 62(21–22), 3453–3473.
- Meissner, K. J., E. D. Galbraith, and C. Völker (2005), Denitrification under glacial and interglacial conditions: A physical approach, *Paleoceanography*, 20, PA3001, doi:10.1029/2004PA001083.
- Montoya, J. P., and J. J. McCarthy (1995), Isotopic fractionation during nitrate uptake by phytoplankton grown in continuous culture, *J. Plankton Res.*, 17(3), 439–464.
- Moore, J. K., M. R. Abbott, J. G. Richman, and D. M. Nelson (2000), The Southern Ocean at the last glacial maximum: A strong sink for atmospheric carbon dioxide, *Global Biogeochem. Cycles*, 14, 455–475.
- Morley, J. J., and J. D. Hays (1983), Oceanographic conditions associated with high abundances of the radiolarian *Cycladophora davisiana*, *Earth Planet. Sci. Lett.*, 66, 63–72.
- Mortlock, R. A., and P. N. Froelich (1989), A simple method for the rapid determination of biogenic iron in pelagic marine sediments, *Deep Sea Res.*, 36, 1415–1426.
- Mortlock, R. A., C. D. Charles, P. N. Froelich, M. A. Zibello, J. Saltzman, J. D. Hays, and L. H. Burckle (1991), Evidence for lower productivity in the Antarctic Ocean during the last glaciation, *Nature*, 351(6323), 220–223.
- Nakatsuka, T., K. Watanabe, N. Handa, E. Matsumoto, and E. Wada (1995), Glacial to interglacial surface nutrient variations of Bering deep basins recorded by $\delta^{13}\text{C}$ and $\delta^{15}\text{N}$ of sedimentary organic matter, *Paleoceanography*, 10, 1047–1061.
- Narita, H., M. Sato, S. Tsunogai, M. Murayama, M. Ikehara, T. Nakatsuka, M. Wakatsuchi, N. Harada, and Y. Ujiié (2002), Biogenic opal indicating less productivity northwestern North Pacific during the glacial ages, *Geophys. Res. Lett.*, 29(15), 1732, doi:10.1029/2001GL014320.
- Needoba, J. A., N. A. Waser, P. J. Harrison, and S. E. Calvert (2003), Nitrogen isotope fractionation in 12 species of marine phytoplankton during growth on nitrate, *Mar. Ecol. Prog. Ser.*, 255, 81–91.
- Nürnberg, D., and R. Tiedemann (2004), Environmental change in the Sea of Okhotsk during the last 1.1 million years, *Paleoceanography*, 19, PA4011, doi:10.1029/2004PA001023.
- Okazaki, Y., K. Takahashi, H. Asahi, K. Katsuki, J. Hori, H. Yasuda, Y. Sagawa, and H. Tokuyama (2005a), Productivity changes in the Bering Sea during the late Quaternary, *Deep Sea Res.*, Part II, 52, 2150–2162.
- Okazaki, Y., K. Takahashi, K. Katsuki, A. Ono, J. Hori, T. Sakamoto, M. Uchida, Y. Shibata, M. Ikehara, and K. Aoki (2005b), Late Quaternary paleoceanographic changes in the southwestern Okhotsk Sea: Evidence from geochemical, radiolarian, and diatom records, *Deep Sea Res.*, Part II, 52, 2332–2350.
- Parekh, P., M. J. Follows, and E. Boyle (2004), Modeling the global ocean iron cycle, *Global Biogeochem. Cycles*, 18, GB1002, doi:10.1029/2003GB002061.
- Pennock, J. R., D. J. Velinsky, D. J. Ludlam, J. H. Sharp, and M. L. Fogel (1996), Isotopic fractionation of ammonium and nitrate during uptake by *Skeletonema costatum*: Implications for $\delta^{15}\text{N}$ dynamics under bloom conditions, *Limnol. Oceanogr.*, 41(3), 451–459.
- Poulsen, N., M. Sumper, and N. Kröger (2003), Biosilica formation in diatoms: Characterizations of native silaffin-2 and its role in silica morphogenesis, *Proc. Natl. Acad. Sci. U.S.A.*, 100(21), 12,075–12,080.
- Price, N. M., B. A. Ahner, and F. M. M. Morel (1994), The equatorial Pacific Ocean—Grazed controlled phytoplankton populations in an iron-limited ecosystem, *Limnol. Oceanogr.*, 39(3), 520–534.
- Pride, C., R. Thunell, D. Sigman, L. Keigwin, M. Altabet, and E. Tappa (1999), Nitrogen isotopic variations in the Gulf of California since the last deglaciation: Response to global climate change, *Paleoceanography*, 14, 397–409.
- Robinson, R. S., B. G. Brunelle, and D. M. Sigman (2004), Revisiting nutrient utilization

- in the glacial Antarctic: Evidence from a new method for diatom-bound N isotopic analysis, *Paleoceanography*, 19, PA3001, doi:10.1029/2003PA000996.
- Robinson, R. S., D. M. Sigman, P. J. DiFiore, M. M. Rohde, T. A. Mashiotta, and D. W. Lea (2005), Diatom-bound $^{15}\text{N}/^{14}\text{N}$: New support for enhanced nutrient consumption in the ice age subantarctic, *Paleoceanography*, 20, PA3003, doi:10.1029/2004PA001114.
- Roden, G. I. (1995), Aleutian Basin of the Bering Sea: Thermohaline, oxygen, nutrient, and current structure in July 1993, *J. Geophys. Res.*, 100, 13,539–13,554.
- Rohling, E. J., P. A. Mayewski, and P. Challenor (2003), On the timing and mechanism of millennial-scale climate variability during the last glacial cycle, *Clim. Dyn.*, 20(2–3), 257–267.
- Sachs, J. P., D. J. Repeta, and R. Goericke (1999), Nitrogen and carbon isotopic ratios of chlorophyll from marine phytoplankton, *Geochim. Cosmochim. Acta*, 63(9), 1431–1441.
- Saitoh, S., I. Takahiro, and K. Sasaoka (2002), A description of temporal and spatial variability in the Berin Sea spring phytoplankton blooms (1997–1999) using satellite multi-sensor remote sensing, *Prog. Oceanogr.*, 55, 131–146.
- Sancetta, C. A. (1983), Effect of Pleistocene glaciation upon oceanographic characteristics of the North Pacific Ocean and Bering Sea, *Deep Sea Res.*, 30, 851–869.
- Sancetta, C. A. (1992), Primary production in the glacial North Atlantic and North Pacific Oceans, *Nature*, 360(6401), 249–251.
- Sancetta, C. A., L. Heusser, L. Labeyrie, A. S. Naidu, and S. W. Robinson (1985), Wisconsin-Holocene paleoenvironment of the Bering Sea: Evidence from diatoms, pollen, oxygen isotopes and clay minerals, *Mar. Geol.*, 62(1–2), 55–68.
- Sarmiento, J. L., and J. R. Toggweiler (1984), A new model for the role of the oceans in determining atmospheric $p\text{CO}_2$, *Nature*, 308(5960), 621–624.
- Sarmiento, J. L., T. M. C. Hughes, R. J. Stouffer, and S. Manabe (1998), Simulated response of the ocean carbon cycle to anthropogenic climate warming, *Nature*, 393(6682), 245–249.
- Sarmiento, J. L., N. Gruber, M. A. Brzezinski, and J. P. Dunne (2004), High-latitude controls of thermocline nutrients and low latitude biological productivity, *Nature*, 427(6969), 56–60.
- Sato, M. M., H. Narita, and S. Tsunogai (2002), Barium increasing prior to opal during the last termination of glacial ages in the Okhotsk Sea sediments, *J. Oceanogr.*, 58, 461–467.
- Seki, O., M. Ikehara, K. Kawamura, T. Nakatsuka, K. Ohnishi, M. Wakatsuchi, H. Narita, and T. Sakamoto (2004), Reconstruction of paleo-productivity in the Sea of Okhotsk over the last 30 kyr, *Paleoceanography*, 19, PA1016, doi:10.1029/2002PA000808.
- Shemesh, A., S. A. Macko, C. D. Charles, and G. H. Rau (1993), Isotopic evidence for reduced productivity in the glacial Southern Ocean, *Science*, 262(5132), 407–410.
- Siegenthaler, U., and T. Wenk (1984), Rapid atmospheric CO_2 variations and ocean circulation, *Nature*, 308(5960), 624–626.
- Sigman, D. M., and E. Boyle (2000), Glacial/interglacial variations in atmospheric carbon dioxide, *Nature*, 407(6806), 859–869.
- Sigman, D. M., L. D. Keigwin, M. A. Altabet, and D. C. McCorkle (1993), The nitrogen isotopic analysis of a deglacial productivity event in the western subarctic Pacific, *Eos Trans. AGU*, 74(16), 185.
- Sigman, D. M., M. A. Altabet, R. Francois, D. C. McCorkle, and J.-F. Gaillard (1999a), The isotopic composition of diatom-bound nitrogen in Southern Ocean sediments, *Paleoceanography*, 14, 118–134.
- Sigman, D. M., M. A. Altabet, D. C. McCorkle, R. Francois, and G. Fischer (1999b), The $\delta^{15}\text{N}$ of nitrate in the Southern Ocean: Consumption of nitrate in surface waters, *Global Biogeochem. Cycles*, 13, 1149–1166.
- Sigman, D. M., M. A. Altabet, D. C. McCorkle, R. Francois, and G. Fischer (2000), The $\delta^{15}\text{N}$ of nitrate in the Southern Ocean: Nitrogen cycling and circulation in the ocean interior, *J. Geophys. Res.*, 105, 19,599–19,614.
- Sigman, D. M., K. L. Casciotti, M. Andreani, C. Barford, M. Galanter, and J. K. Böhlke (2001), A bacterial method for the nitrogen isotopic analysis of nitrate in seawater and freshwater, *Anal. Chem.*, 73(17), 4145–4153.
- Sigman, D. M., S. J. Lehman, and D. W. Oppo (2003), Evaluating mechanisms of nutrient depletion and ^{13}C enrichment in the intermediate-depth Atlantic during the last ice age, *Paleoceanography*, 18(3), 1072, doi:10.1029/2002PA000818.
- Sigman, D. M., S. L. Jaccard, and G. H. Haug (2004), Polar ocean stratification in a cold climate, *Nature*, 428(6978), 59–63.
- Skinner, L. C., and N. J. Shackleton (2005), An Atlantic lead over Pacific deep-water change across termination I: Implications for the application of the marine isotope stage stratigraphy, *Quat. Sci. Rev.*, 24, 571–580.
- Stuiver, M., P. J. Reimer, E. Bard, J. W. Beck, G. S. Burr, K. A. Hughen, B. Kromer, F. G. McCormac, J. v. d. Plicht, and M. Spurk (1998), INTCAL98 Radiocarbon age calibration 24,000–0 cal BP, *Radiocarbon*, 40, 1041–1083.
- Swift, D. M., and A. P. Wheeler (1992), Evidence of an organic matrix from diatom biosilica, *J. Phycol.*, 28(2), 202–209.
- Tanaka, S., and K. Takahashi (2005), Late Quaternary paleoceanographic changes in the Bering Sea and the western subarctic Pacific based on radiolarian assemblages, *Deep Sea Res., Part II*, 52, 2131–2149.
- Temois, Y., K. Kawamura, L. Keigwin, N. Ohkouchi, and T. Nakatsuka (2001), A biomarker approach for assessing marine and terrigenous inputs to the sediments of Sea of Okhotsk for the last 27,000 years, *Geochim. Cosmochim. Acta*, 65(5), 791–802.
- Thunell, R. C., and A. B. Kepple (2004), Glacial-Holocene $\delta^{15}\text{N}$ record from the Gulf of Tehuantepec, Mexico: Implications for denitrification in the eastern equatorial Pacific and changes in atmospheric N_2O , *Global Biogeochem. Cycles*, 18, GB1001, doi:10.1029/2002GB002028.
- Thunell, R. C., D. M. Sigman, F. Muller-Karger, Y. Astor, and R. Varela (2004), Nitrogen isotope dynamics of the Cariaco Basin, Venezuela, *Global Biogeochem. Cycles*, 18, GB3001, doi:10.1029/2003GB002185.
- Timmermans, K. R., M. A. van Leeuwe, J. T. M. de Jong, R. M. L. McKay, R. F. Nolting, H. J. White, J. van Ooyen, M. J. W. Swagerman, H. Kloosterhuis, and H. J. W. de Baar (1998), Iron stress in the Pacific region of the Southern Ocean: Evidence from enrichment bioassays, *Mar. Ecol. Prog. Ser.*, 166, 27–41.
- Toggweiler, J. R. (1999), Variation of atmospheric CO_2 by ventilation of the ocean's deepest water, *Paleoceanography*, 14, 571–588.
- Toggweiler, J. R. and S. Carson (1995), What are the upwelling systems contributing to the ocean's carbon and nutrient budgets?, in *Upwelling in the Ocean: Modern Processes and Ancient Records*, edited by C. P. Summerhayes et al., pp. 337–360, John Wiley, Hoboken, N. J.
- Toggweiler, J. R., and B. Samuels (1995), Effect of Drake Passage on the global thermohaline circulation, *Deep Sea Res., Part I*, 42, 477–500.
- Toggweiler, J. R., J. L. Russell, and S. R. Carson (2006), Midlatitude westerlies, atmospheric CO_2 , and climate change during the ice ages, *Paleoceanography*, 21, PA2005, doi:10.1029/2005PA001154.
- Tsuda, A., et al. (2003), A mesoscale iron enrichment in the western subarctic Pacific induces a large centric diatom bloom, *Science*, 300(5621), 958–961.
- van Geen, A., R. G. Fairbanks, P. Dartnell, M. McGann, J. V. Gardner, and M. Kashgarian (1996), Ventilation changes in the northeast Pacific during the last deglaciation, *Paleoceanography*, 11, 519–528.
- van Geen, A., Y. Zheng, J. M. Bernhard, K. G. Cannariato, J. Carriquiry, W. E. Dean, B. W. Eakins, J. D. Ortiz, and J. Pike (2003), On the preservation of laminated sediments along the western margin of North America, *Paleoceanography*, 18(4), 1098, doi:10.1029/2003PA000911.
- Wang, Z., L. A. Mysak, and J. F. McManus (2002), Response of the thermohaline circulation to cold climates, *Paleoceanography*, 17(1), 1006, doi:10.1029/2000PA000587.
- Waser, N. A. D., D. H. Turpin, P. J. Harrison, B. Nielsen, and S. E. Calvert (1998), Nitrogen isotope fractionation during the uptake and assimilation of nitrate, nitrite, and urea by a marine diatom, *Limnol. Oceanogr.*, 43(2), 215–224.
- Winton, M. (1997), The effect of cold climate upon North Atlantic Deep Water formation in a simple ocean-atmosphere model, *J. Clim.*, 10(1), 37–51.
- Wu, J., S. E. Calvert, and C. S. Wong (1997), Nitrogen isotope variations in the northeast subarctic Pacific: Relationships to nitrate utilization and trophic structure, *Deep Sea Res., Part I*, 44, 287–314.
- Zheng, Y., A. van Geen, R. F. Anderson, J. V. Gardner, and W. E. Dean (2000), Intensification of the northeast Pacific oxygen minimum zone during the Bölling-Allerød warm period, *Paleoceanography*, 15, 528–536.

B. G. Brunelle and D. M. Sigman, Department of Geosciences, Princeton University, Princeton, NJ 08544, USA. (brunelle@princeton.edu)

M. S. Cook and L. D. Keigwin, Department of Marine Geology and Geophysics, Woods Hole Oceanographic Institution, Woods Hole, MA 02543-1050, USA.

G. H. Haug, B. Plessen, and G. Schettler, Geoforschungszentrum Potsdam, Telegrafenberg, D-14473 Potsdam, Germany.

S. L. Jaccard, Department of Earth and Ocean Sciences, University of British Columbia, 6270 University Boulevard, Vancouver, BC, Canada V6T 1Z4.